

Black Hole and Cosmological Particle Production in Schwarzschild de Sitter

Yue Qiu and Jennie Traschen

Department of Physics
University of Massachusetts, Amherst, MA 01003, USA

Email: yqiu@physics.umass.edu, traschen@physics.umass.edu

Abstract

We compute the spectra and total fluxes of quantum mechanically produced particles crossing the black hole and cosmological horizons in Schwarzschild de Sitter (SdS). Particle states are defined with respect to well-behaved, Kruskal coordinates near the horizons, and as a consequence we find that these spectra are generally non-thermal. The non-thermal Bogoliubov coefficient for a vacuum fluctuation near the black hole horizon to produce a particle that crosses the cosmological horizon is shown to equal to the convolution of two thermal coefficients, one at the cosmological temperature and one at the black hole temperature, weighted by the transmission coefficient for wave propagation in static SdS coordinates. In this sense virtual thermal propagation underlies the production process. This representation leads to the useful result that the geometric optics approximation is reliable when used together with a low frequency cut-off determined by the transmission coefficient. The large black hole limit is a quasi-equilibrium situation as both temperatures approach the common value of zero, the particle spectra become equal, and both emissions are exponentially suppressed. Small black holes radiate as thermal bodies and absorb a tiny flux of cosmological particles. The behavior of the quantum fluctuations on the horizons is seen to be consistent with the Schottky anomaly behavior of classical gravitational fluctuations.

I. INTRODUCTION

Hawking taught us that the formal identification of the surface gravity κ_b of a black hole with a temperature, as suggested by the first law of black hole mechanics [1], is realized quantum mechanically [2]. Considering an asymptotically flat black hole that is initially in the vacuum state of a quantum field, he calculated that far from the black hole and at late times there is a flux of quantum mechanical particles. Famously, the spectrum of the radiation is thermal with temperature $2\pi T_b = \kappa_b$. Subsequently reference [3] showed that the cosmological horizon in de Sitter also leads to the thermal emission of quantum particles with temperature $2\pi T_c = \kappa_c$, where is the magnitude of the cosmological horizon surface gravity.

In a black hole spacetime with positive Λ there is particle production due to both the black hole and cosmological horizons. This is an intriguing situation, since the two surface gravities are not typically equal, which is at odds with our usual expectations of thermal equilibrium. Of course, unequal temperatures is also a feature of asymptotically flat black holes if one assigns $T_\infty = 0$ to the asymptotically flat region, and is consistent with the fact that black holes evaporate. Thermal properties of Schwarzschild-de Sitter (SdS) black holes were explored in [3] using general considerations. Particle production for charged de Sitter black holes was computed in [4] which focused on the the special case of $|Q| = M$ when both temperatures are equal and nonzero. It was found that the spectra for $|Q| = M$ black holes is not thermal. In this paper we greatly expand on the work of [4]. We calculate the particle spectra and the total particle production rates for both the black hole and cosmological horizons in Schwarzschild-de Sitter. With the exception of radiation from small black holes, we find that these spectra are non-thermal. This perhaps unexpected result arises from our choice of particle states. To compute particle fluxes crossing the horizons, either being absorbed by the black hole or flowing with the expanding universe across the cosmological horizon, it is necessary to use modes for the particle states that are well-behaved on the horizons. The natural choice for the time coordinate is to use an affine parameter along null geodesics, that is, Kruskal coordinates. This choice constitutes

a generalization of the Unruh vacuum in Schwarzschild [5] to SdS [6].

The motivation for interest in particles that are well defined on the horizons was, in part, to explore quantum aspects of the Schottky anomaly of SdS black holes, discussed in a companion paper [7]. Schottky behavior refers to peaks in the specific heat dE/dT and in dS/dT for certain statistical mechanics systems. In SdS one finds that there is a Schottky-type peak in dS_{tot}/dT_b , where $S_{tot} = S_b + S_c$ is the total gravitational entropy, and a trough in dM/dT_b ¹. These extrema can be understood as a result of suppression of classical fluctuations in S_{tot} and M at high and low temperatures [7]. Since quantum fluctuations are always present in the system, particle production in SdS is a natural way to extend the classical considerations, and the high and low temperature limits are studied in detail here. Since entropy is a property of the horizon geometry one needs to use particle states that are well behaved on the horizons. There have been several recent papers that analyze closely related questions. The stress-energy tensor for the Unruh state in de Sitter has been computed [8] using Kruskal modes on the horizon, and it would be interesting to see how those results extend to SdS. A Schottky anomaly for AdS black holes has recently been studied in [9][10], and similar features were computed for AdS black holes in two-dimensional dilaton gravity [11]. Another recent paper studies the Schottky anomaly in SdS and analyzes the system as a heat engine [10].

Our results contrast with another recent calculation of the black hole and the cosmological particle production in SdS [12], where a particular set of states are chosen such that both spectra *are* thermal at the temperatures T_b and T_c . In this case, the particle states used are not well behaved on the horizons, so the calculations are done near the horizons. Is there a consistency problem between the differing results? Consider the standard Minkowski vacuum with particles defined by freely falling observers. Recall that Rindler observers, *i.e.* ones who move with constant acceleration in this vacuum, detect a thermal flux of particles with temperature proportional to their acceleration. The temperature can be tuned by changing the acceleration. So clearly the form observed for a particle spectrum depends on who does the measurement, so there is no contradiction. Nonetheless, it is reasonable to ask

¹ There is a minimum in $M(T_b)$ rather than a maximum due to the negative specific heat.

how these qualitatively different results are related. To analyze this question, we introduce the notion of a spectral amplitude, which is the complex quantity that leads to the (real) particle spectrum. We show in section (IV) that the spectral amplitude for the Kruskal particles is equal to an integral over frequencies of the product of thermal amplitudes at temperatures T_b and T_c , weighted by an appropriate transmission coefficient. Hence the amplitude for produced particles crossing one horizon or the other can be thought of as composed of “intermediate” thermal state interactions.

Particle production calculations are limited by the difficulty of solving the wave equation in a curved spacetime. For Schwarzschild, Hawking argued that the geometric optics approximation can be used since particle production is a high frequency process. However, SdS has two scales which means that it is less clear what “high” frequency means. The wave propagation needs to be more carefully studied to choose accurate frequency cut-offs. We find that introducing the intermediate states just referred to is very useful in sorting out the cut-offs, as the transmission coefficients for the waves necessarily enter, and these encode how modes behave as a function of frequency.

The family of SdS spacetimes interpolates between very small black holes, whose geometry near the black hole horizon is like Schwarzschild, and large black holes with area that approaches the area of the cosmological horizon. Equipped with physical cut-offs we are able to compute the black hole and cosmological particle spectra for this range of black hole areas. The total rates of particles crossing each horizon is then found, which requires some interesting considerations about the emission and absorption geometries. Small black holes with $T_b \gg T_c$ share the black hole instability of Schwarzschild and emit particles in the expected thermal spectrum, which is compensated for by only a tiny amount of absorption of cosmological particles. In the large black hole limit both temperatures approach the common value of zero in a quasi-equilibrium state and the spectra become equal, but particle production is exponentially suppressed. Hence these spacetimes illustrate a rich variety of complicated behavior.

This paper is organized as follows. In Section (II) we review relevant properties of SdS,

choose the particle states, and develop needed formulas to compute the particle spectra and total particle production rates. In Section (III) the geometric optics approximation is used to evaluate the spectra in terms of an undetermined cut-off frequency. Exact formula for the Bogoliubov amplitudes as the convolution of thermal amplitudes is derived in Section (IV A) and physical frequency cut-offs are then inferred. The relevant density of states is derived in Section (V) and then the spectra and production rates are computed, with a focus on the small and large black hole limits. Section (VI) presents our conclusions and open questions. Several details of the calculations are given in the appendices.

II. SETTING UP THE CALCULATION

We study a massless scalar field in SdS, and consider the causally connected region outside the black hole and inside the cosmological horizon as shown in Figure 1. Compared to an asymptotically flat black hole the boundaries at past and future null infinity are replaced by the past and future cosmological horizons. Particles crossing the future cosmological horizon are interpreted as coming from the black hole, and those entering the black hole are interpreted as coming from the cosmological horizon. In this section we define the particle states and establish the formulae for the particle spectra (19) and the total rate of particle production (21). Some details are moved to Appendix (A).

A. Schwarzschild-deSitter basics

The metric of Schwarzschild- deSitter spacetime in static patch coordinates (t, r) is

$$ds^2 = -f(r)dt^2 + \frac{1}{f(r)}dr^2 + r^2d\Omega^2 \quad (1)$$

where

$$f(r) = 1 - \frac{2M}{r} - \frac{r^2}{l_c^2} = -\frac{1}{r_c^2}(r - r_c)(r - r_b)(r + r_c + r_b) \quad (2)$$

where $r_c > r_b$ are the locations of the cosmological and black hole horizons respectively, and $\frac{1}{3}\Lambda = 1/l_c^2$. The two parametrizations are related by

$$M = \frac{r_b r_c (r_b + r_c)}{2(r_b^2 + r_c^2 + r_b r_c)}, \quad l_c^2 = r_b^2 + r_c^2 + r_b r_c \quad (3)$$

The horizon surface gravities (or temperatures) are given by $2\pi T_h = \kappa_h = |f'(r_h)|/4\pi$, or

$$\kappa_b = \frac{(r_c - r_b)(2r_b + r_c)}{2l_c^2 r_b}, \quad \kappa_c = \frac{(r_c - r_b)(2r_c + r_b)}{2l_c^2 r_c} \quad (4)$$

Note that κ_h is used to denote the *magnitude* of the black hole and cosmological horizon surface gravities, for h respectively. For the metric to describe a black hole horizon rather than a naked singularity, there is a maximum value to the mass

$$M \leq M_{max} = \frac{l_c}{3\sqrt{3}} \quad (5)$$

which ensures that there are two positive roots to f . For fixed l_c , as M increases from zero to its maximum, A_b increases and A_c decreases to the common value of $4\pi l_c^2/3$. The total entropy $S = \frac{1}{4}(A_b + A_c)$ is largest for small black holes for which $T_b \rightarrow \infty$ and $T_c \rightarrow 1/l_c$. The entropy is smallest when the two horizons approach each other, in which case both temperatures go to zero. Hence S increases with increasing T_b unlike Schwarzschild black holes. On the other hand, the specific heat is still negative as with $\Lambda = 0$. The existence of a maximum size black hole is an important distinction from the $\Lambda \leq 0$ cases. For fixed l_c the full parameter space is explored by studying $0 < r_b < l_c/\sqrt{3}$, which will be referred to as small and large black holes.

The first laws in SdS [13] describe the influence of perturbations of one horizon on the other horizon and on the mass,

$$\delta M = T_b \delta S_b - V_b \frac{\delta \Lambda}{8\pi}, \quad \delta M = -T_c \delta S_b - V_c \frac{\delta \Lambda}{8\pi} \quad (6)$$

Here V_h is the thermodynamic volume associated with each horizon which in SdS has the simple form $V_h = \frac{4}{3}\pi r_h^3$. Taking the difference of the two equations gives a first law that only involves quantities in the causal diamond

$$T_b \delta S_b + T_c \delta S_c = -V \delta \Lambda \quad (7)$$

where $V = \frac{4}{3}\pi(r_c^3 - r_b^3)$ is the thermodynamic volume between the horizons. Note that we are using the conventions that temperatures are positive and use κ_h for the magnitude of the surface gravity at each horizon. This will avoid absolute value signs in expressions below. Features of black hole thermodynamics in deSitter, including approaches to temperature, entropy, and conserved charges, are studied in [14–28]. Features of black hole thermodynamics in an expanding universe are contained in [29–31]. In addition to the classical gravitational perturbations described by the first laws (6) and (7), there are quantum fluctuations in the matter fields, even if the classical values are zero. Our goal is to compute the quantum mechanical fluxes of particles crossing each horizon due to the presence of the other horizon.

B. Choice of early and late time particle modes

The first step is to choose modes functions associated with creation and annihilation operators that define what is meant by a particle. We use the formalism for quantum field theory in curved spacetime presented in [32] and more specifically for black holes in [33]. Additional treatments are contained in [34] [35]. The Penrose diagram for the portion of SdS bounded by the black hole and cosmological horizons is shown in Figure 1. Choosing the boundary conditions on the mode functions is guided by the following physical considerations. In Hawking’s original calculation, with $\Lambda = 0$, he considered gravitational collapse to form a black hole, and so the past black horizon \mathcal{H}_b^- was covered up by the collapsing star. This has the advantage that at early times the geometry is close to flat, and the system starts in the usual Minkowski vacuum. At late times and far from the black hole, spacetime is close to Minkowski, so there is again a natural choice of positive frequency modes. Note that observers near future null infinity who use the Killing time coordinate to define particles are freely falling. It was later shown by Unruh [5] that the particle production results are the same if the calculation is done in the extended Schwarzschild spacetime by defining states on \mathcal{H}_b^- with respect to the geodesic null Kruskal coordinate U_b . This is a satisfying result not only because it is simpler to work in the extended spacetime than a

collapsing star, but also because it illustrates that freely falling observers with coordinates defined by the geodesics are a choice that gives physically sensible results. Unlike the far field, near the black hole geodesic time is not time along the Killing flow.

Consider the other limit, de Sitter spacetime with no black hole ($M = 0$). There is a significant body of research about choosing vacuum states in deSitter and inflationary cosmologies, see *e.g.* [8, 36–46], and for a pedagogical treatment and further references see [32]. The quantum mechanical production of particles in inflation has been computed in multiple contexts and compared in detail to observations. In the cosmological setting, the picture is that a portion of an early FRW spacetime goes through a phase transition which changes the effective equation of state to that of a cosmological constant, so the spacetime is not de Sitter before a certain time or outside the inflating bubble. The past cosmological horizon is covered up by an earlier FRW period. Similar to the fact that a collapsing star covers up \mathcal{H}_b^- , the entry to inflation covers up the past cosmological horizon \mathcal{H}_c^- . Reference [6] recently computed properties of an Unruh state in two-dimensional de Sitter, using Kruskal coordinates to define modes on \mathcal{H}_c^- and \mathcal{H}_b^+ .²

Markovic and Unruh [47] extended the work of [5] for Schwarzschild to two dimensional SdS, and computed the two-point function and stress energy tensor, focusing on the observations of static observers, who are shown to see a near thermal stress energy. They also demonstrated that there is agreement between using Kruskal boundary conditions on \mathcal{H}_c^- and \mathcal{H}_b^+ in the extended two-dimensional SdS spacetime, and the results in a spacetime in which a collapsing star covers up \mathcal{H}_b^- . Reference [17] built upon the analysis of [47] and examined the expectation value of the stress-energy tensor for several choices of SdS states in two dimensions. The response of particle detectors in black hole and in cosmological spacetimes was analyzed in [48]. Our choice is the same as equation (26) of [17] in two dimensions, though in four dimensions there are differences (see footnote #2). Reference [17] finds that static particle detectors detect thermal fluxes. Hence the results of [47], [17],

² In the two-dimensional case there is no scattering, and so boundary conditions on a portion of the past Cauchy surface can be replaced with boundary conditions on a portion of the future Cauchy surface, and generalizations of the “Unruh state” are often presented in this way. However in four dimensions there is scattering and these formulations are not the same.

and [12] make a consistent package, and report on thermal properties of several quantities measured by static observers

In contrast, as mentioned above, we define particles near each horizon with respect to Kruskal coordinates of freely falling observers. The issue of static time *vs.* geodesic time particles will be returned to in Section (IV B), and connections made between our results to this earlier work. Proceeding, we assume that the proper physics is captured by doing the calculation in the extended SdS spacetime and defining positive frequency on \mathcal{H}_c^- with respect to the geodesic Kruskal coordinate V_c and on the \mathcal{H}_b^- with respect to U_b , as was done in previous work of one of the authors [4]. Note that using these free-fall coordinates to define particle states on both horizons when $\Lambda > 0$ is a simple generalization of Unruh's analysis for Schwarzschild black holes [5]. The primary distinction from the other treatments is that we focus on produced Kruskal particles, rather than quantities measured by static, accelerating, observers.

Particles produced due to a horizon in one part of a spacetime are observed in another part of the spacetime. In Schwarzschild, particles interpreted as coming from the black hole are detected at late times at future null infinity \mathcal{I}^+ . In SdS \mathcal{I}^+ is a spacelike surface to the future of \mathcal{H}_c^+ . We will restrict our attention to the causal diamond for SdS shown in Figure 1, in which the boundaries \mathcal{I}^\pm of an asymptotically flat spacetime are replaced by the cosmological horizons \mathcal{H}_c^\pm . Of course, in SdS the spacetime extends beyond \mathcal{H}_c^+ and it would be interesting to compute the particle production observed by cosmological observers in the far field, but in this paper we focus on the bath of particles near each horizon, due to the presence of the other horizon.

the modes are solutions to the wave equation

$$g^{ab}\nabla_a\nabla_b f = g^{ab}\nabla_a\nabla_b p = 0 \tag{8}$$

and set of modes $f_\omega^h, f_\omega^{*h}$ and $p_\omega^h, f_\omega^{*h}$ forms an orthonormal basis in the conserved Klein-Gordon inner product,

$$(f_\omega^h, f_\nu^{h'}) = \delta(\omega - \nu)\delta^{hh'} \tag{9}$$

where

$$(h, g) \equiv -i \int_{\Sigma} d^3x \sqrt{|\gamma|} n^a (h \partial_a g^* - g^* \partial_a h) \quad (10)$$

Here Σ is a Cauchy surface with unit normal n^a and $\sqrt{|\gamma|}$ is the volume element of the induced metric on Σ .

The null geodesic, or Kruskal, coordinates near each horizon are related to the static patch null coordinate $v = t + r^*$ and $u = t - r^*$ where $dr^* = dr/f$, by

$$U_c = \frac{1}{\kappa_c} e^{\kappa_c u}, \quad V_c = -\frac{1}{\kappa_c} e^{-\kappa_c v}, \quad U_b = -\frac{1}{\kappa_b} e^{-\kappa_b u}, \quad V_b = \frac{1}{\kappa_b} e^{\kappa_b v} \quad (11)$$

On each horizon the appropriate Kruskal coordinate is equal to zero, see Figure 1.

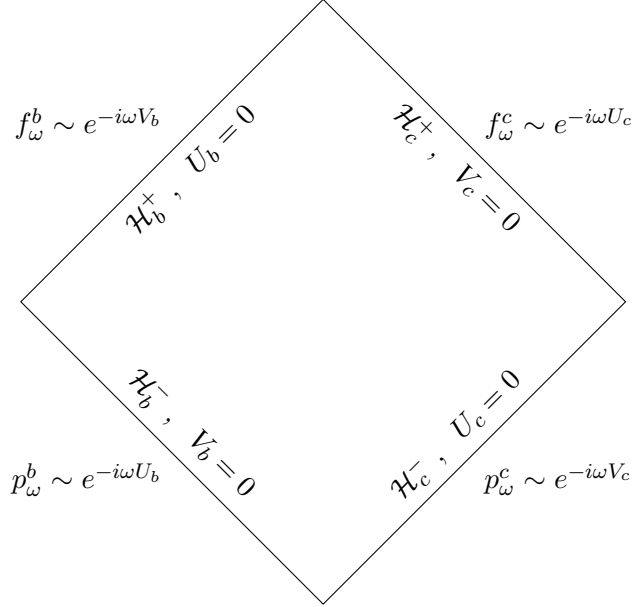


FIG. 1. The "Causal Diamond", or static patch of SdS, bounded by the past and future black hole and cosmological horizons. Positive frequency particle modes are defined with respect to the appropriate Kruskal coordinate on each portion of the boundary as indicated.

The union of the past black hole and cosmological horizons is a Cauchy surface for the diamond on which the boundary conditions for the early time modes. Let p_ω^b denote a mode that has positive frequency ω with respect to the affine coordinate U_b on the past black

hole horizon b and that vanishes on the past cosmological horizon,

$$\begin{aligned} p_{\omega lm}^b &= \frac{Y_{lm}(\Omega)}{\sqrt{4\omega r_b}} e^{-i\omega U_b} && \text{on } \mathcal{H}_b^- \\ &= 0 && \text{on } \mathcal{H}_c^- \end{aligned} \tag{12}$$

where the $Y_{lm}(\Omega)$ are the spherical harmonics on S^2 . The modes are normalized in the Klein-Gordon innerproduct (10). One technical point is that, for example, the Kruskal coordinate U_b ranges between $-\infty < U_b \leq 0$ on \mathcal{H}_b^- . Under the Kruskal extension that surface is continued into the black hole region, covered by the other half-line $0 \leq U_b < \infty$. The inner product for the p_ω^b is taken along the entire range of the Kruskal coordinate³. However, except for the normalization, the behavior of the modes in the extended region will not be relevant for our calculations, which examine what happens in the causal diamond and on its boundaries. Analogous comments pertain to the normalization of the other sets of modes.

Similarly, p_ω^c denotes a mode that has positive frequency ω with respect to the affine coordinate V_c on the past cosmological horizon c and that vanishes on the past black hole horizon. A second, late time Cauchy surface is the union of the future black hole and cosmological horizons, and we denote the late time modes functions by f . The mode f_ω^c has positive frequency ω with respect to V_c on the future cosmological horizon and vanishes on the future black hole horizon, and conversely for f_ω^b . The boundary conditions are summarized in Figure 1.

The field Φ can be decomposed in either the basis of the past or the future modes,

$$\begin{aligned} \Phi &= \sum_{lm} \int d\omega (a_{\omega lm}^b p_{\omega lm}^b + a_{\omega lm}^c p_{\omega lm}^c + h.c.) \\ &= \sum_{lm} \int d\omega (b_{\omega, lm}^b f_{\omega lm}^b + b_{\omega lm}^c f_{\omega lm}^c + h.c.) \end{aligned} \tag{13}$$

³ We would like to thank Paul Anderson for useful conversations on this issue.

Here $a_{\omega,lm}^{c\dagger}$ creates a particle at early times defined with respect to the Kruskal coordinate U_c near the past cosmological horizon, and $a_{\omega,lm}^{b\dagger}$ creates a particle at early times defined with respect to the Kruskal coordinate V_b near the past black hole (white hole) horizon. Likewise, $b_{\omega lm}^{b\dagger}$ and $b_{\omega lm}^{c\dagger}$ create late time particles near the black hole and future cosmological horizons respectively. Unless needed, we will suppress the angular quantum numbers l, m .

C. Formalism: black hole and cosmological particle spectra and total production rates

Assume that the spacetime is initially in the early time vacuum defined by

$$a_{\omega}^b|0\rangle = a_{\omega}^c|0\rangle = 0 \quad (14)$$

Our goal is to compute the number of late time particles which are created by $b^{b\dagger}$ near the future cosmological horizon, which are interpreted by local observers as coming from the black hole. Likewise, we will compute the late time particles created by $b^{c\dagger}$ crossing the black hole horizon, which are interpreted as being produced by the cosmological horizon. So, compared to an asymptotically flat black hole, in this analysis the boundary at future (past) null infinity is replaced by the future (past) cosmological horizon.

Each late time mode can be expanded in terms of the early time basis and *vice-versa*. Let

$$f_{\omega}^c = \int d\omega' [\alpha_{\omega\omega'}^b p_{\omega'}^b + \beta_{\omega\omega'}^b p_{\omega'}^{b*} + A_{\omega\omega'}^c p_{\omega'}^c + B_{\omega\omega'}^c p_{\omega'}^{c*}] \quad (15)$$

and similarly for the mode f_{ω}^b with the labels on the right hand side interchanged ($b \rightarrow c$, $c \rightarrow b$). The mode-mixing Bogoliubov coefficients $\alpha_{\omega\omega'}$ and $\beta_{\omega\omega'}$ give the amplitude for scattering an in-modes with positive frequency ω to out-modes with positive frequency ω' and negative frequency $-\omega'$ respectively, the latter leading to particle production. The $A_{\omega\omega'}$ and $B_{\omega\omega'}$ coefficients are needed in the basis expansion and are given by the overlap of a wave that enters the diamond through the past cosmological horizon, scatters off the geometry, and leaves through the future cosmological horizon. This is a classical scattering

process and does not contribute significantly to the the particle production, but does enter into the normalization condition (A6) below.

The Bogoliubov coefficients in (15) are computed by using the Klein-Gordon inner product,

$$\begin{aligned}\alpha_{\omega\omega'}^b &= (f_\omega^c, p_{\omega'}^b) & \beta_{\omega\omega'}^b &= -(f_\omega^c, p_{\omega'}^{b*}) = -i\alpha_{\omega, -\omega'} \\ A_{\omega\omega'}^c &= (f_\omega^c, p_{\omega'}^c) & B_{\omega\omega'}^c &= -(f_\omega^c, p_{\omega'}^{c*})\end{aligned}\tag{16}$$

The expressions for the coefficients $\alpha_{\omega\omega'}^c, \beta_{\omega\omega'}^c, A_{\omega\omega'}^b$ and $B_{\omega\omega'}^b$ are obtained by interchanging the labels b and c . Then the relation between the in and out particle operators follows from (15) and (13), which give

$$b_\omega^c = \int d\omega' \left[\alpha_{\omega\omega'}^{b*} a_{\omega'}^b - \beta_{\omega\omega'}^{b*} a_{\omega'}^{b\dagger} + A_{\omega\omega'}^{c*} a_{\omega'}^c - B_{\omega\omega'}^{b*} a_{\omega'}^{c\dagger} \right]\tag{17}$$

and similarly for the operator b_ω^b , with the labels on the right hand side interchanged ($b \rightarrow c, c \rightarrow b$).

In equation (13) the field Φ is expanded in mode functions labeled by a continuous frequency parameter ω , which is convenient for calculations and we will be used here. However, to get formulae for physically relevant quantities such as the number of particles produced per unit volume, one needs to use properly normalized wave packets. Since many of the equations – but not all – repeat those already presented with discrete rather than continuous indices, we include the steps in Appendix (A). The frequencies are integer-indexed as $\omega_j = j/R$ where R is a length scale associated with the density of states, see (20). The key output is that the probability of horizon h producing a late-time particle with frequency ω_j which is observed crossing horizon h' ,

$$N_{\omega_j}^h = \sum_k |\beta_{jk}^h|^2, \quad h = b, c\tag{18}$$

becomes

$$N_\omega^h = \frac{1}{R} \int d\omega' |\beta_{\omega\omega'}^h|^2\tag{19}$$

in the continuous basis, where $\sum_k = R \int d\omega'$ has been used. Note the important dimensional factor of $1/R$ that multiplies the integral using the continuous basis functions, and that N_ω^h is dimensionless.

The angular momentum eigenvalue l has been mostly suppressed, but now we need to include the density of states. The total number of particles produced with frequency ω_j is the product of N_{ω_j} times the density of states $\rho(\omega_j) = \sum_l (2l + 1)$. In the continuous basis functions one has

$$\rho(\omega) = \sum_l (2l + 1) (d\omega R) \quad (20)$$

The number of particles produced per unit time results from integrating (19) over ω and dividing by R , which cancels the R in the density of states,

$$n_h = \sum_l (2l + 1) \int d\omega N_\omega^h \quad (21)$$

This has dimensions $(length)^{-1}$ as it should. The energy emitted per unit time E_h^ϕ in the ϕ -particles is gotten by including another factor of ω in the integrand of (21).

Lastly, one needs to fix R that arises in the density of states, and appears in (19). Reference [32] computes the particle production due to a shell that collapses to a black hole, and take R to be the light travel time from the shell to a distant sphere where the particle flux is measured. In analogy, we will take R to be the light travel distance between the two horizons. Studying null geodesics one finds that $R = (r_c - r_b)$, so for small black holes $R \simeq l_{cos}$. For large black holes this distance is going to zero, and expressed in terms of the surface gravity one finds $R \simeq \kappa l_{cos}^2$, where we have set $\kappa = \kappa_b \simeq \kappa_c \rightarrow 0$.

III. PARTICLE PRODUCTION IN THE GEOMETRIC OPTICS LIMIT

Particle production results when a mode that is positive frequency with respect to the modes on one horizon propagates into a mixture of positive and negative frequency modes on the other different horizon. The $\alpha_{\omega\omega'}^b$ mode mixing integral for production due to the

black hole horizon is given by the inner product equation (16), which we will evaluate on the past Cauchy surface. Since p^b vanishes on \mathcal{H}_c^- , this reduces to an integral over the past black hole horizon. Hence we need the solutions for the future modes f^c on \mathcal{H}_b^- . Hawking argues [2] that since the main effect comes from high frequency modes the wave equation can be solved in the geometric optics approximation, in which the wave f^c propagates unchanged on a surface of constant phase $U_b = \text{constant}$ to intersect \mathcal{H}_b^- . Explicitly, using (11) to trace a line of constant U or V in the causal diamond above, the Kruskal coordinates on the boundaries are related to each other by

$$U_c = \frac{1}{\kappa_c} (-\kappa_b U_b)^{-\frac{\kappa_c}{\kappa_b}} \quad \text{and} \quad V_b = \frac{1}{\kappa_b} (-\kappa_c V_c)^{-\frac{\kappa_b}{\kappa_c}} \quad (22)$$

A mode f_ω^c goes like $e^{-i\omega U_c}$ on \mathcal{H}_c^+ , so on \mathcal{H}_b^- it goes like $e^{-i(\omega/\kappa_c)(-\kappa_b U_b)^{-\kappa_c/\kappa_b}}$. Substituting into the inner product (10) gives

$$\alpha_{\omega\omega'}^b = \frac{1}{4\pi\sqrt{\omega\omega'}\kappa_b} \int_0^\infty dx e^{-i\frac{\omega'}{\kappa_b}x} e^{-i\frac{\omega}{\kappa_c}x^{-\kappa_c/\kappa_b}} \left(\omega' + \omega x^{-\frac{\kappa_T}{\kappa_b}} \right) \quad (23)$$

where $\kappa_T = \kappa_b + \kappa_c$. The integral for $\alpha_{\omega\omega'}^b$ only goes over \mathcal{H}_b^- which is the half-line $-\infty < U_b \leq 0$, since no portion of the mode f_ω^b comes out of the black hole. It is straightforward to check that the integral for $\alpha_{\omega\omega'}^c$, for the particle production due to the cosmological horizon, is given by interchanging κ_c and κ_b in (25).

It is interesting to compare $\alpha_{\omega\omega'}^b$ to the corresponding integral for an asymptotically flat black hole, which is given by setting $\epsilon = 0$ in equation (78), and can be evaluated in terms of Γ -functions as given in (31). The Minkowski null coordinate used to define particles at future null infinity is related by a single red shift to the Kruskal coordinates that define particles near the black hole horizon. In SdS the inner product is between two sets of Kruskal modes, which involves a Kruskal-to-static coordinate redshift followed by a static-to-Kruskal blueshift given in equation (11). The sequence of red and blue shifts gives a more complicated integrand, and produces a spectrum that is not thermal.

For generic values of the surface gravities these integrals can be evaluated using the method

of stationary phase,

$$I(k) = \int e^{i\phi(t)/k} f(t) \underset{k \rightarrow 0}{\simeq} e^{i\phi(t_s)/k} f(t_s) e^{\text{Sign}(\phi''(t_s)) \frac{i\pi}{4}} \sqrt{\frac{2\pi k}{|\phi''(t_s)|}} \quad (24)$$

where t_s is the point of stationary phase $\phi'(t_s) = 0$ which is assumed to be in the range of integration. Applying (24) to equation (23) with $\phi(x) = -(\omega' x \kappa_c / \kappa_b + x^{-\lambda} \omega)$ and $x_0 = (\omega / \omega')^{\kappa_b / \kappa_T}$ gives

$$\alpha_{\omega\omega'}^b \simeq -\frac{\sqrt{2}e^{-\frac{i\pi}{4}}}{\sqrt{\pi\kappa_T}(\omega^{\kappa_c}\omega'^{\kappa_b})^{1/2\kappa_T}} \exp\left[-i\frac{\kappa_T}{\kappa_b\kappa_c}(\omega'^{\kappa_c}\omega^{\kappa_b})^{1/\kappa_T}\right] \quad (25)$$

As summarized in equation (16) one then analytically continues in ω' to get $\beta_{\omega\omega'}^b = -i\alpha_{\omega,-\omega'}^b$. Viewed as a complex function of ω' , $\alpha_{\omega\omega'}$ is analytic in the lower half ω' -plane, since it is the Fourier transform of the function (25), which vanishes in the lower half x -plane. Hence when analytically continuing the branch cut that arises must be put in the upper half ω' plane, and $\omega' \rightarrow -\omega' = e^{-i\pi}|\omega'|$, giving

$$\beta_{\omega\omega'}^b \simeq -i\frac{\sqrt{2}e^{-\frac{i\pi}{4}}e^{i\pi\kappa_b/2\kappa_T}}{\sqrt{\pi\kappa_T}(\omega^{\kappa_c}\omega'^{\kappa_b})^{1/2\kappa_T}} \exp\left[-\frac{\kappa_T}{\kappa_b\kappa_c}(\omega'^{\kappa_c}\omega^{\kappa_b})^{1/\kappa_T}\left(i\cos\pi\frac{\kappa_c}{\kappa_T} + \sin\pi\frac{\kappa_c}{\kappa_T}\right)\right] \quad (26)$$

This Bogoliubov coefficient gives the mixing of negative frequency modes the black hole horizon with positive frequency cosmological modes, that is, a cosmological Kruskal observer near \mathcal{H}_c^+ interprets the resulting flux as particles coming from the black hole. To get the reverse situation of particles detected near the black hole produced from the cosmological horizon, one can check that κ_b and κ_c are simply interchanged in (25),

$$\alpha_{\omega\omega'}^c(\kappa_b, \kappa_c) = \alpha_{\omega\omega'}^b(\kappa_c, \kappa_b) \quad (27)$$

Interestingly, after using the stationary phase approximation, the integral for the number of produced particles (19) can be done easily, giving

$$N_\omega^b = \frac{2}{\pi\omega R} \frac{\mathcal{K}}{\kappa_c} \exp\left[-\frac{1}{\mathcal{K}}(\omega^{\kappa_b}\omega_0^{\kappa_c})^{1/\kappa_T}\right] \quad , \quad (28)$$

where

$$\mathcal{K} = \frac{\kappa_c \kappa_b}{2\kappa_T \sin(\pi \kappa_c / \kappa_T)} \rightarrow \begin{cases} \kappa_b / 2\pi, & \kappa_b \gg \kappa_c \\ \kappa / 4 & \kappa = \kappa_b \rightarrow \kappa_c \rightarrow 0 \end{cases} \quad (29)$$

Hence \mathcal{K} is equal to the black hole temperature in the small black hole limit, and proportional to the common temperature for large black holes. The spectrum for the cosmological particles N_ω^c is obtained by interchanging κ_b and κ_c . Note that the quantity \mathcal{K} is invariant under interchanging κ_b and κ_c .

This is as far as we can go without specifying the cut-off frequency in the integrall over ω' to get N_ω . In Schwarzschild there is only one scale, so necessarily $\omega_0 \propto 1/r_b$. However SdS has two scales, so a better understanding of the process is needed, which we now turn to.

IV. EXACT TREATMENT: THERMAL AMPLITUDES, NON-THERMAL AMPLITUDES, AND PHYSICAL CUT-OFFS

Consider an early time mode p_ω^b (or p_ω^c) that has boundary conditions set on the past horizons. The inner product for a Bogoliubov coefficient is an integral over a Cauchy surface. So to compute the mode mixing with a late time mode one needs to know the solution for p_ω^b on the future horizons, and this is where the technical challenges arise. Following Hawking [2], the wave equation was solved in the geometric optics limit in the previous section. We next show that the geometric optics approximation plus judicious choices for the low frequency cut-offs and for the limits on the sum over angular momentum quantum number l in the integrals for N_ω^h and n_h give accurate results for the particle production. If one could solve the wave equation then the solutions for the modes would incorporate such restrictions, as will be clear in results below. But finding solutions is a hard problem so approximation techniques must be used. So the goal of this section is to derive an exact expression for the Bogoliubov coefficients that includes the effects of scattering of the modes. This also leads to interesting physics.

A. Building blocks: thermal amplitudes

In the particle production calculation the real valued spectrum N_ω results from squaring the complex quantity $\beta_{\omega\omega'}$ and summing over the contributions from all states ω' . In analogy with the relation between a wave function and the expectation value of an operator, we introduce the notion of $\beta_{\nu\nu'}$ as the ‘‘amplitude for a spectrum’’, that is, the complex function whose integrated norm gives the spectrum,

$$N_\nu = \frac{1}{R} \int d\nu' |\beta_{\nu\nu'}|^2 \quad (30)$$

The amplitude depends on the background geometry and on the choices of the two bases of past and future modes that are being compared. An important reference case is the asymptotically flat Schwarzschild black hole [2]. Then the amplitude is the inner product between black hole *Kruskal* modes with outgoing null time coordinate U , and asymptotically *Minkowski* plane waves near future null infinity \mathcal{I}^+ with outgoing null time coordinate u . These dependences will be indicated as $\beta_{\nu\nu'}^{AF}(K_b, M; \kappa_b)$ where K_b refers to Kruskal coordinates near the black hole horizon and M refers to freely falling Minkowski coordinates. In the geometric optics approximation Hawking showed that the amplitude has a nice expression in terms of Gamma-functions,

$$\begin{aligned} \beta_{\nu\nu'}^{AF}(K_b, M; \kappa_b) &= e^{-\pi\nu/\kappa_b} \alpha_{\nu\nu'}^{AF}(K_b, M; \kappa_b) , \\ \text{where } \alpha_{\nu\nu'}^{AF}(K_b, M; \kappa_b) &= -\frac{1}{\pi\kappa_b\sqrt{\nu\nu'}} \left(\frac{i\nu'}{\kappa_b}\right)^{-i\nu/\kappa_b} \Gamma\left(1 + \frac{i\nu}{\kappa_b}\right) \end{aligned} \quad (31)$$

This basic ‘‘building block’’ for Schwarzschild can be thought of as a *thermal* spectral amplitude, in the sense that the resulting spectrum is, famously, thermal,

$$N_\nu^{AF}(K_b, M; \kappa_b) = \frac{1}{R} \int d\nu' |\beta_{\nu\nu'}^{AF}(K_b, M; \kappa_b)|^2 = \frac{\gamma_\nu^{AF}}{e^{\nu/2\pi\kappa_b} - 1} \quad (32)$$

where γ_ν^{Sch} is the classical scattering amplitude in the Schwarzschild geometry and $\kappa_b = 1/2r_b$ is the black hole surface gravity in Schwarzschild.

A second relevant example studied recently [12] is the SdS black hole with the choice of modes chosen to closely parallel the Schwarzschild calculation. The past modes on \mathcal{H}_b^- are defined with respect to Kruskal time U_b , but unlike our calculation, the future modes are defined with respect to the static patch null coordinate u on a null surface near the cosmological horizon. It is found [12] that

$$\beta_{\nu\nu'}^{b,SdS}(K_b, M; \kappa_b) = \beta_{\nu\nu'}^{AF}(K_b, M; \kappa_b) \quad (33)$$

One should note that the two surface gravities κ_b on each side of (33) do not have the same expressions in terms of r_b and l , since $\Lambda = 0$ on the right hand side. It follows that the black hole spectrum for Kruskal to static modes is thermal [12],

$$N_{\nu}^{b,SdS}(K_b, M; \kappa_b) = \frac{1}{R} \int d\nu' |\beta_{\nu\nu'}^{b,SdS}(K_b, M; \kappa_b)|^2 = \frac{\gamma_{\nu}^{SdS}}{e^{\nu/2\pi\kappa_b} - 1} \quad (34)$$

where γ_{ν}^{SdS} is now the classical scattering amplitude in the SdS geometry. Hence when the static coordinate plane waves are chosen for the future modes, the difference in the amplitudes between SdS and Schwarzschild only appears in the different greybody factors, for the same value of κ_b . Reference [12] also derives an analogous expression for the cosmological particle production in SdS, choosing the past modes to be defined with respect to the ingoing Kruskal coordinate V_c on \mathcal{H}_c^- and the future modes defined with respect to the static patch ingoing null coordinate $v = t + r_*$ near \mathcal{H}_b^+ . The resulting Bogoliubov coefficient has the same functional form as that for asymptotically flat black hole emission with κ_b replaced by κ_c ,

$$\beta_{\nu\nu'}^{c,SdS}(K_c, M; \kappa_c) = \beta_{\nu\nu'}^{AF}(K_b, M; \kappa_c) \quad (35)$$

and so again leads to a thermal spectrum for the cosmological particle production at $T_c = \kappa_c/(2\pi)$.

B. SdS emission as a convolution of thermal amplitudes

We next derive an exact formula for the amplitude in SdS defined with respect to Kruskal modes on the past *and* future horizons, which will turn out to be an integral over ther-

mal amplitudes $\beta_{\nu\nu'}^{b,SdS}(K_b, M; \kappa_b)$ and $\beta_{\nu\nu'}^{c,SdS}(K_c, M; \kappa_c)$ weighted by the transmission coefficients for wave propagation in SdS. We will find that in general N_ω^b and N_ω^c are not thermal, but through this formula can be viewed as an integral over a continuous set of pre-thermal interactions. The analysis takes advantage of the fact that the wave equation is separable in the static patch (t, r_*) coordinates⁴. While analytic solutions are not known in the (t, r_*) coordinates either one replaces the problem of solving a partial differential equation with solving a standard one-dimensional scattering problem, whose solutions can be written in terms of transmission $T_{\nu l}$ and scattering $S_{\nu l}$ coefficients that can be evaluated by various approximation techniques. Including these coefficients in the calculation yields an exact expression for $\beta_{\omega\omega'}^b$ that has an interesting and useful form in terms of simpler *thermal* amplitudes.

To proceed, we make use of a third set of mode functions k_ω as “intermediate states”. In the static patch coordinates of the metric (1), solutions to the wave equation $\square k_\omega = 0$ are separable as

$$k_{\nu l}(r_*, t) = \frac{\psi_{\nu l}(r_*)e^{-i\nu t}}{r\sqrt{2\pi\nu}}Y_{lm} \quad (36)$$

where $dr_* = dr/f$. The black hole horizon is at $r_* \rightarrow -\infty$ and the cosmological horizon at $r_* \rightarrow \infty$. k_ν is a solution to the wave equation if ψ_ν is a solution to the ordinary differential equation

$$\partial_{r_*}^2 \psi_\nu + (\omega^2 - V(r_*)) \psi_\nu = 0 \quad (37)$$

where the potential is

$$V = V_0 + V_l = \frac{f}{r} \frac{df}{dr} - \frac{l(l+1)}{r^2} \quad (38)$$

The l -independent part of the potential goes to zero exponentially fast in the tortoise coordinate near each horizon,

$$V_0 \rightarrow \kappa_b^2 e^{\kappa_b r_*}, \quad \text{near } \mathcal{H}_b; \quad V_0 \rightarrow -\kappa_c^2 e^{-\kappa_c r_*}, \quad \text{near } \mathcal{H}_c \quad (39)$$

V_0 also is equal to zero at $r_0^3 = l^2 M = \frac{1}{2} r_b r_c (r_c + r_b)$ where $df/dr = 0$, so V_0 is positive for $r_b < r < r_0$ where f' is positive, and is negative for $r_0 > r > r_c$. This reflects the competition between the attraction of the black hole and the cosmological expansion.

⁴ We thank Paul Anderson for pointing out this approach

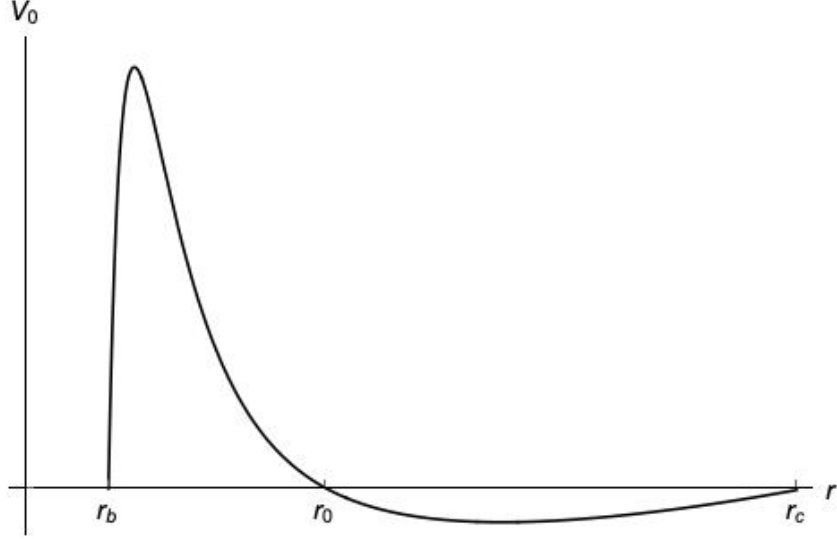


FIG. 2. Plot of the potential V_0 . There is a potential barrier and a potential well in Schwarzschild de Sitter space-time.

As before, we suppress the angular momentum index unless needed for clarity. Consider solutions for k_ν that are plane waves in the outgoing null coordinate $u = t - r_*$ near \mathcal{H}_b^- , and vanish on \mathcal{H}_c^- . Part of the wave then propagates across the potential barrier and leaves through \mathcal{H}_c^+ with amplitude $T_{\nu l}$, and a portion scatters back into \mathcal{H}_b^+ with amplitude $S_{\nu l}$, so

$$k_{\nu l} \rightarrow \begin{cases} 0, & \mathcal{H}_c^- \\ \frac{1}{\sqrt{2\pi\nu r_b}} e^{-i\nu u} Y_{lm} & \mathcal{H}_b^- \\ \frac{1}{\sqrt{2\pi\nu r_c}} T_{\nu l} e^{-i\nu u} Y_{lm} & \mathcal{H}_c^+ \\ \frac{1}{\sqrt{2\pi\nu r_b}} S_{\nu l} e^{-i\nu v} Y_{lm} & \mathcal{H}_b^+ \end{cases} \quad (40)$$

where $|T_\nu|^2 + |S_\nu|^2 = 1$. At high frequencies the wave is well over the barrier and $T_\nu \rightarrow 1$, $S_\nu \rightarrow 0$. This is regime in which geometric optics is applicable. At low frequencies most of the wave is scattered back by the potential and $T_\nu \rightarrow 0$, $S_\nu \rightarrow 1$.

Again, we start with the expansion of the future modes f_ω^c in terms of the past modes p_ω^b given in equations (15) and (16). The new ingredient is to also expand the k_ν in terms of

the p_ω^b , and the f_ω^c in terms of the k_ν ,

$$\begin{aligned} k_\nu &= \int_0^\infty d\nu' [J_{\nu\nu'} p_{\nu'}^b + L_{\nu\nu'} p_{\nu'}^{b*}] \\ f_\omega^c &= \int_0^\infty d\nu' [M_{\omega\nu'} k_{\nu'} + N_{\omega\nu'} k_{\nu'}^*] \end{aligned} \quad (41)$$

hence

$$f_\omega^c = \int_0^\infty d\nu' d\nu [p_{\nu'}^b (M_{\omega\nu'} J_{\nu\nu'} + N_{\omega\nu'} L_{\nu\nu'}^*) + p_{\nu'}^{b*} (M_{\omega\nu'} L_{\nu\nu'} + N_{\omega\nu'} J_{\nu\nu'}^*)] \quad (42)$$

which implies via (15) that

$$\alpha_{\omega\nu'}^b = \int_0^\infty d\nu (M_{\omega\nu} J_{\nu\omega'} + N_{\omega\nu} L_{\nu\omega'}^*) \quad (43)$$

The analogue of the terms with the coefficients $A_{\omega\nu'}^c$ and $B_{\omega\nu'}^c$ which appear in (15) have been dropped since as mentioned earlier they make subdominant contributions to particle production. The new expansion coefficients are given by the inner products

$$J_{\nu\nu'} = (k_\nu, p_{\nu'}^b), \quad M_{\omega\nu'} = (f_\omega^c, k_{\nu'}), \quad \text{and} \quad L_{\nu\nu'} = -iJ_{\nu,-\nu'}, \quad N_{\omega\nu'} = -iM_{\omega,-\nu'} \quad (44)$$

We evaluate $J_{\nu\nu'}$ on \mathcal{H}_b^- ,

$$\begin{aligned} J_{\nu\nu'} &= \frac{1}{2\sqrt{2\pi\kappa_b}\sqrt{\nu\omega'}} \int_0^\infty dx e^{i\nu \ln x/\kappa_b} e^{-i\omega' x/\kappa_b} \left(\omega' + \frac{\nu}{x} \right) \\ &= \frac{-i}{\sqrt{2\pi\kappa_b}\sqrt{\nu\omega'}} \left(\frac{i\omega'}{\kappa_b} \right)^{-i\nu/\kappa_b} \Gamma\left(1 + i\frac{\nu}{\kappa_b}\right) \\ &= \frac{i}{\sqrt{2}} \alpha_{\nu\omega'}^{AF}(K_b, M; \kappa_b) \end{aligned} \quad (45)$$

and evaluation of $M_{\omega\nu'}$ on \mathcal{H}_c^+ gives

$$\begin{aligned} M_{\omega\nu} &= \frac{-iT_\nu^*}{\sqrt{2\pi\kappa_c}\sqrt{\omega\nu}} \left(\frac{i\omega}{\kappa_c} \right)^{-i\nu/\kappa_c} \Gamma\left(1 + i\frac{\nu}{\kappa_c}\right) \\ &= \frac{i}{\sqrt{2}} T_\nu^* \alpha_{\nu\omega}^{AF}(K_b, M; \kappa_c) \end{aligned} \quad (46)$$

The transmission coefficient T_ν^* has entered through the future boundary behavior of k_ν . Combining (43), (45), and (46) gives

$$\begin{aligned} \alpha_{\omega\omega'}^b(K_b, K_c; \kappa_b, \kappa_c) &= \int_{-\infty}^{\infty} d\nu T_\nu^* \alpha_{\nu\omega}^{AF}(K_c, M; \kappa_c) \alpha_{\nu\omega'}^{AF}(K_b, M; \kappa_b) \\ &= -\frac{1}{2\pi^2 \kappa_b \kappa_c \sqrt{\omega\omega'}} \int d\nu \frac{T_\nu^*}{\nu} \Gamma\left(1 + i\frac{\nu}{\kappa_b}\right) \left(\frac{i\omega'}{\kappa_b}\right)^{-i\nu/\kappa_b} \Gamma\left(1 + i\frac{\nu}{\kappa_c}\right) \left(\frac{i\omega}{\kappa_c}\right)^{-i\nu/\kappa_c} \end{aligned} \quad (47)$$

where the two terms in (43) have been combined by extending range of integration over the entire ν axis and using $T_\nu^* = T_{-\nu}$. Analytically continuing in ω' as discussed earlier, $\omega' \rightarrow |\omega'|e^{-i\pi}$, and substituting the relations (31) and (33) gives the desired expression for $\beta_{\omega\omega'}^b$

$$\beta_{\omega\omega'}^b(K_b, K_c; \kappa_b, \kappa_c) = \int_{-\infty}^{\infty} d\nu T_\nu^* \alpha_{\nu\omega}^{AF}(K_c, M; \kappa_c) \beta_{\nu\omega'}^{AF}(K_b, M; \kappa_b) \quad (48)$$

An analogous expression holds for the amplitude for the cosmological particle production.

What can be learned from the result (48)? At the beginning of this paper we argued that to study particle production at the horizons, particles must be defined with respect to modes that are well behaved on the horizons. In general, the resulting spectra will not thermal, see (28) (or (66) and (67)). However, the relation (48) shows that the *amplitude* for the spectrum can be written as a convolution of *thermal amplitudes*. To get an observable one must take the complex modulus of $\beta_{\omega\omega'}^b$, which does not just depend on the squares of the thermal amplitudes, but depends on interference effects in the integral (48), which is expected in a quantum process. What is perhaps less expected is that the quantum interactions between the horizons can be summarized in such a simple form.

V. SPECTRA, DENSITY OF STATES, AND PRODUCTION RATES

While (47) and (48) provide physical insight, there does not seem to be a route for evaluating the integrals exactly. So we will derive an approximate expression for (47) again using the

method of stationary phase (24). The details are in Appendix (B), where it is shown that after three applications of stationary phase the triple integral for $\alpha_{\omega\omega'}^b$ reduces to the geometric optics result (25) except that there is now a factor of the transmission coefficient multiplying the expression. So the result for $\beta_{\omega\omega'}^b$ is also the same as the geometric optics result (26) multiplied by T_ν ,

$$|\beta_{\omega\omega'}^b|^2 \simeq \frac{2|T_{\sigma l'}|^2}{\pi\kappa_T(\omega^{\kappa_c}\omega'^{\kappa_b})^{1/\kappa_T}} \exp\left[-\frac{2}{\mathcal{K}}(\omega'^{\kappa_c}\omega^{\kappa_b})^{1/\kappa_T}\right] \delta_{ll'} \quad (49)$$

where σ is the complex frequency

$$\sigma = (\omega'^{\kappa_c}\omega^{\kappa_b})^{1/\kappa_T} e^{-i\pi\kappa_c/\kappa_T} \quad (50)$$

and $\mathcal{K} = \kappa_c\kappa_b[2\kappa_T\sin(\pi\kappa_c/\kappa_T)]^{-1}$, see (29) for the limiting behaviors of \mathcal{K} . The complex phase factor in σ results from the analytic continuation in ω' to obtain $\beta_{\omega\omega'}^b$, that leads to the decaying exponential in $|\beta_{\omega\omega'}^b|^2$.

The integral over ω' gives

$$N_{\omega l}^b = \delta_{ll'} \frac{2}{\pi\omega R} \frac{\mathcal{K}}{\kappa_c} \int_0^\infty dx |T_{x'l'}|^2 e^{-x} \quad , \quad x' = \sigma(x) = x\mathcal{K}e^{-i\pi\kappa_c/\kappa_T} \quad (51)$$

We have restored the l, l' indices to remind the reader that there is dependence on the angular momentum, as this will be important in the next section. The spectrum for cosmological particles N_ω^c is obtained by interchanging κ_b and κ_c .

Equations (49) and (51) are equal to the corresponding quantities derived using geometric optics times factors that depend on the transmission coefficient.

The (simpler) geometric optics method gave the result (28) for N_ω^b , which involves a low frequency cut-off ω_0 . Comparing (28) to (51) implies that ω_0 should be chosen equal to the frequency where the transmission coefficient changes from zero to one. More precisely, we have shown is that the geometric optics method plus choosing the cut-off to be in the transition regime of the transmission coefficient $T_{\omega l}$ gives a good approximation for the Bogoliubov coefficients. This is one of our main results.

A. Relevant density of states and processed formulae

We now turn to the issue of finding the transition frequency for the transmission coefficient as just discussed. We also identify additional conditions on ω and l that must be incorporated before integrating over the product of the density of states times N_ω^h to get n_h .

Even without detailed knowledge of the behavior of the transmission coefficient $T_{\omega'l}$, equation (69) contains useful information. We know that $|T_{\omega'l}|^2$ goes to one when the wave is well over the potential V and goes to zero when ω' is sufficiently small compared to the maximum of V . The potential (38) has a portion V_0 that is independent of the angular momentum of the field, plus an angular momentum barrier $V_l = l(l+1)/r^2$. A tractable approximation is that a mode with frequency ω' is over the barrier when its frequency squared is greater than the height of each portion of the potential, *i.e.*, when $\omega' > \omega_0$, where

$$\omega_0^2 \simeq \text{Max} \left(\text{max}(V_0), \frac{l^2}{r_m^2} \right) \quad (52)$$

Here r_m is the location of the maximum of V . We will refer to ω_0 as the cut-off frequency, and approximate the spectrum by replacing $T_{\omega'l}$ with a step-function at the cutoff. Then the black hole spectrum (51) reduces to the expression derived using geometric optics (28), with the important addition that now the cut-off is specified in (52)

For Schwarzschild the maximum of V_0 is at $r_m = 4r_b/3$, and for large black holes necessarily $r_m \simeq r_b$, so we will simply approximate $r_m \simeq r_b$. For small black holes the geometry near the black hole is close to Schwarzschild, and one finds that $\text{max}(V_0) \simeq \kappa_b^2$. This is simply the physical result that the wave is over the barrier if its frequency is greater than the black hole temperature. On the other hand, for large black holes when $\kappa_b \rightarrow \kappa_c \rightarrow 0$, one finds that the maximum of the potential goes to zero like $\text{max}(V_0) \simeq l_c^{1/2} \kappa^3$. Hence,

$$\omega_0 \simeq \frac{\kappa_b}{2\pi} \quad , \quad \text{small bhs} \quad \text{and} \quad \omega_0 \simeq l_c^{1/4} \kappa^3 \quad , \quad \text{large bhs} \quad (53)$$

These considerations apply equally well to production of particles by the black hole or by the cosmological horizon, since V is fixed for a given geometry.

To get the total rate of particle production n_h in (21) from $N_{\omega l}$ one sums over l and integrates over ω . There are constraints on the range of both l and ω , as follows. Start by writing equation (47) for $\alpha_{\omega\omega'}^b$ as

$$\alpha_{\omega\omega'}^b = F(\omega, \omega'; \kappa_b, \kappa_c) \quad (54)$$

Since $\alpha_{\omega\omega'}^c$ results from interchanging the labels b and c one has

$$\alpha_{\omega\omega'}^c = F(\omega, \omega'; \kappa_c, \kappa_b) \quad (55)$$

Inspection of (47) shows that F is symmetric under interchange of ω, ω' and κ_b, κ_c ,

$$F(\omega, \omega'; \kappa_b, \kappa_c) = F(\omega', \omega; \kappa_c, \kappa_b) \quad (56)$$

which translates to

$$\alpha_{\omega\omega'}^b = \alpha_{\omega'\omega}^c \quad (57)$$

Since we have established that the functions $\alpha_{\nu\mu}^b$ and $\alpha_{\nu\mu}^c$ vanish when the second frequency index is less than ω_0 , equation (57) implies that there is also a cut-off at ω_0 in the first index of these functions.

Next, before summing over the angular momenta in the density of states the condition on l in (52) must be incorporated. For fixed ω , the condition implies that $l < \omega r_b$, hence

$$\int_{\omega_0} d\omega \sum_{l=0}^{[\omega r_b]} (2l+1) N_{\omega}^b \simeq r_b^2 \int_{\omega_0} d\omega \omega^2 N_{\omega}^b \quad (58)$$

It is satisfying that doing the sum over l brings in the familiar factor of ω^2 times a *length*² in the density of states.

In addition to the condition that the wave is over the barrier, there are features of the absorption and scattering geometry that need to be taken into account. For an oscillation to be detected as a wave by measurements inside the causal diamond its wavelength must be less than the propagation distance, that is, $\omega > 1/(r_c - r_b)$. For small black holes this is not an additional restriction compared to (52), but for large black holes we have

$$\omega > \omega_1 = \frac{1}{r_c - r_b} \simeq \frac{1}{l_c^2 \kappa}, \quad \text{large } bhs \quad (59)$$

which is a much higher cut-off than $\omega_0 = \sqrt{\max(V)} \simeq l_c^{1/4} \kappa^{3/4}$. Since the condition (59) is about a classical detection process it applies to the integration over frequencies of the spectrum to get n_h , but not to the first integration over the frequencies of the amplitudes. It applies to both n_c and n_b since emission and absorption processes become symmetrical between the two horizons for large black holes.

However not everything is symmetric when the black hole is small. Any wave propagating outwards from the black hole will cross the cosmological horizon, but a wave propagating inwards from the cosmological horizon needs to have a wavelength $\lambda < r_b$, or it simply slashes over the black hole and propagates out through the cosmological horizon. A small length λ corresponds to a large angular momentum number l as $\lambda \simeq r_c/l$, so for a mode to be absorbed by the black hole

$$l > \frac{r_c}{r_b} \quad (60)$$

This is an important constraint for small black holes with $r_c/r_b \gg 1$. For larger black holes it is not a significant restriction, which corresponds to the fact that the black hole is indeed in the way of most waves. Combining (60) and (52) gives the following allowed range of l and more stringent cutoff ω_1 for a small black hole to absorb cosmological particles,

$$r_b \omega > l > \frac{r_c}{r_b} = \frac{1}{\epsilon} \gg 1, \quad \text{and} \quad \omega_1 = \kappa_b \frac{r_c}{r_b} = \frac{\kappa_b}{\epsilon} \gg \kappa_b, \quad (\text{small bh}) \quad (61)$$

where small black holes are defined by $\epsilon = r_b/r_c \ll 1$.

Let us close by summarizing the sum over contributing states. We use the notation ω_0 for the cut-off derived from the condition that the wave is over V_l , which is the lower limit for the integration over ω' to get N_ω . We use ω_1 for a possibly more stringent cut-off that includes additional geometric considerations:

(1) Cosmological particles absorbed by small black holes: The total number of particles per unit time absorbed by the horizon of a small black hole is given by

$$n_c = \int_{\omega_1} d\omega \left[(r_b \omega)^2 - \left(\frac{r_c}{r_b} \right)^2 \right] N_\omega^c, \quad \omega_1 = \omega_0 = \frac{\kappa_b}{\epsilon} \quad (62)$$

The two terms in the square brackets come from the upper and lower limits in the sum over l .

(2) Black hole particles: The total number of particles emitted by the black hole per unit time as measured at the cosmological horizon is given by

$$n_b = \frac{A_b}{4\pi} \int_{\omega_1} d\omega \omega^2 N_\omega^b \quad (63)$$

where

$$\omega_1 = \omega_0 \simeq \frac{\kappa_b}{2\pi} \quad \text{small bhs} , \quad \omega_1 \simeq \frac{1}{l_c^2 \kappa} \quad \text{large bhs} \quad (64)$$

(3) Large black holes: The black hole and cosmological particle production becomes symmetrical with $N_\omega^c \simeq N_\omega^b$ and $n_c \simeq n_b$ with

$$n_h = \frac{A_b}{4\pi} \int_{\omega_1} d\omega \omega^2 N_\omega^h , \quad \omega_1 \simeq \frac{1}{l_c^2 \kappa} \quad (65)$$

B. Particle spectra and total production rates

For ease of comparison, we repeat the formula for the black hole particle spectrum (28) derived using geometric optics,

$$N_\omega^b = \frac{2}{\pi\omega R} \frac{\mathcal{K}}{\kappa_c} \exp\left[-\frac{1}{\mathcal{K}}(\omega^{\kappa_b} \omega_0^{\kappa_c})^{1/\kappa_T}\right] , \quad \omega > \omega_0 \quad (66)$$

The cosmological particle spectra is obtained by interchanging κ_b and κ_c which gives

$$N_\omega^c = \frac{2}{\pi\omega R} \frac{\mathcal{K}}{\kappa_c} \exp\left[-\frac{1}{\mathcal{K}}(\omega^{\kappa_c} \omega_0^{\kappa_b})^{1/\kappa_T}\right] , \quad \omega > \omega_0 \quad (67)$$

where

$$\mathcal{K} = \frac{\kappa_c \kappa_b}{2\kappa_T \sin(\pi\kappa_c/\kappa_T)} \quad (68)$$

(see (29) for the limiting behavior of \mathcal{K}). The results of Section (IV A) imply that it is a good approximation to use these geometric optics expressions with the appropriate cut-off ω_0 for N_ω^h and ω_1 for n_h , given in equations (62) to (65). The total black hole particle production rates is gotten by substituting N_ω^b into (63),

$$n_b = \frac{A_b \omega_0^{-2\kappa_c/\kappa_b}}{4\pi^2 R \sin(\pi\kappa_c/\kappa_T)} \frac{1}{\mathcal{K}^{2\kappa_T/\kappa_b}} \Gamma\left(\frac{2\kappa_T}{\kappa_b}, \frac{\omega_0^{\kappa_c/\kappa_T} \omega_1^{\kappa_b/\kappa_T}}{\mathcal{K}}\right) \quad (69)$$

where $\Gamma(s, q) = \int_q dy y^{s-1} \exp[-y]$ is the incomplete Gamma function. The production rate of cosmological particles is gotten by interchanging the labels b and c , giving

$$n_c = \frac{A_b \omega_0^{-2\kappa_b/\kappa_c}}{4\pi^2 R \sin(\pi\kappa_c/\kappa_T)} \frac{1}{\mathcal{K}^{2\kappa_T/\kappa_c}} \Gamma\left(\frac{2\kappa_T}{\kappa_c}, \frac{\omega_0^{\kappa_c/\kappa_T} \omega_1^{\kappa_b/\kappa_T}}{\mathcal{K}}\right) \quad (70)$$

Equations (66) through (70) give the spectra and total rate of particle production from the black hole and cosmological horizons, as defined with respect to freely falling frames crossing the cosmological and black hole horizons respectively, and constitute one of the main results of this paper. An important feature is that in general the spectra are not thermal. When applying these formulae one needs to use the appropriate cut-off frequencies listed in (62) through (65). Explicit formulae for the cut-off are given in the limits of small and large black holes. To find the cut-off ω_0 for a general black hole further analysis of the potential V is needed, which we defer to future work. Next we focus on the two limits.

Large black holes:

In the large black hole limit the mass is going to its maximum value, both horizon areas approach the value $4\pi l_c^2/3$, the surface gravities are going to zero, $\kappa = \kappa_b \rightarrow \kappa_c \rightarrow 0$, and the two spectra approach the common form

$$N_\omega^c \simeq N_\omega^b = \frac{1}{2\pi\omega l_c^2 \kappa} \exp\left[-\frac{4\omega^{1/2} l_c^{1/4}}{\kappa^{1/4}}\right], \quad \omega > \frac{1}{l_c^2 \kappa} \quad (71)$$

where $R = r_c - r_b \simeq l_c^2 \kappa$ has been used. The spectrum is non-thermal, and has the same $\sqrt{\omega}$ dependence in the exponent as was found for $Q = M$ black holes in de Sitter [4], in which case the cosmological and black hole temperatures are also equal but non-zero. The restriction to higher frequencies comes from (65) and the contributing frequencies are in the tail of the distribution. Hence production is highly suppressed.

Likewise, the total number of particles produced per unit time goes to zero very rapidly as κ goes to zero.

$$n_b \simeq n_c \simeq \frac{1}{6\pi l} \frac{e^{-4/(l_c \kappa)^{3/4}}}{(l_c \kappa)^{9/4}} \quad (72)$$

To find the differences in the two spectra one needs to include corrections to the temperatures. So large SdS black holes are in a quasi-equilibrium state with the particle absorption

by each horizon almost balancing its emission, and both processes exponentially suppressed.

Small black holes: Small black holes are defined by the condition that

$$\epsilon = \kappa_c/\kappa_b \ll 1 \quad (73)$$

In this regime, $r_b \simeq 1/(2\kappa_b)$, $\kappa_c \simeq 1/l_c$, and $R \simeq l_c$. For particle production by the black hole the cut-off frequency is $\omega_0 = \kappa_b/(2\pi)$ and (66) becomes

$$N_\omega^b = \frac{1}{\pi^2 \omega l_c} \kappa_b e^{-2\pi\omega/\kappa_b} \quad (74)$$

which is the expected (high frequency part of a) thermal spectrum for the black hole emission at temperature $T_b = \kappa_b/2\pi$. One might wonder why one does not get the exact Bose-Einstein spectrum, a point that we return to at the end of this section. Next, the total number of particles emitted per unit time (69) reduces to

$$n_b \simeq \frac{A_b}{16\pi^5 \kappa_c R} \kappa_b^3 \simeq \frac{\kappa_b}{16\pi^4} \quad (75)$$

Note that the first expression for n_b has the standard dependence on area and temperature for thermal radiation of entropy by an emitter of area A and temperature T , $n \propto AT^3$, and that the emitted energy goes like AT^4 . The last expression for n_b in (75) has a non-standard temperature dependence because the area of a black hole has the non-standard property that it depends on temperature.

Turning now to the cosmological particles, in the small black hole limit the cut-off (62) is $\omega_0 = \kappa_b/(2\pi\epsilon) \gg \kappa_b/(2\pi)$, so (67) becomes

$$N_\omega^c = \frac{1}{\pi^2 \omega} e^{-y} \quad , \quad y(\omega) \simeq \frac{1}{\epsilon} (\epsilon l_c \omega)^\epsilon \rightarrow \frac{1}{\epsilon} (l_c \omega)^\epsilon \quad (76)$$

The spectrum has a slow but non-zero exponential decay, which is critical to have a finite total particle production n_c . The small black hole limit of n_c in (70) is⁵

$$n_c \sim \frac{A_b \kappa_b^2}{16\pi^2 l_c \pi} (\epsilon)^{2/\epsilon} \Gamma\left(\frac{2}{\epsilon}, \frac{1}{\epsilon}\right) = \frac{e^{-\kappa_b/\kappa_c}}{8\pi^4 (\pi - 1) l_c} \quad (77)$$

⁵ One finds that a higher order expansion of N_ω^c is needed if the $\epsilon \rightarrow 0$ limit is taken before integrating.

where the asymptotic form of the incomplete Gamma function $\Gamma(s, q) \simeq q^s e^{-q}/(s(\pi - 1))$ for $q \gg 1$ has been used. Not surprisingly, the absorption of cosmological particles by a very small black hole is very small.

Small black holes following Hawking:

For small black holes one would expect to recover the Planck spectrum plus corrections, rather than just the high frequency tail found in (74). For small black holes κ_b gets arbitrarily large, and one might worry that the stationary phase approximation is not accurate since it assumes that the frequencies are the largest scales. So as a check we return to the integral (25) for $\alpha_{\omega\omega'}^b$ and using $\epsilon = \frac{\kappa_c}{\kappa_b} \ll 1$ expand $x^{-\epsilon} \simeq (1 - \epsilon \ln x)$ in the phase factor. This puts the integrand into a form where the leading term in the ϵ expansion matches the Schwarzschild black hole studied by Hawking [2]

$$\begin{aligned} \alpha_{\omega\omega'}^b &\simeq \frac{e^{-i\omega/\kappa_c}}{4\pi\kappa_b\sqrt{\omega\omega'}} \int_0^\infty dx \left(\omega' + \frac{\omega}{x^{1+\epsilon}} \right) x^{i\omega/\kappa_b} e^{-i\omega'x/\kappa_b} \\ &= \frac{e^{-i\omega/\kappa_c}}{4\pi i\kappa_b\sqrt{\omega\omega'}} \left(\frac{i\omega'}{\kappa_b} \right)^{-i\omega/\kappa_b} \left(\Gamma\left(1 + \frac{i\omega}{\kappa_b}\right) + \left(\frac{i\omega'}{\kappa_b} \right)^\epsilon \Gamma\left(1 - \epsilon + \frac{i\omega}{\kappa_b}\right) \right) \end{aligned} \quad (78)$$

When $\epsilon = 0$ this reduces to the result for $\alpha_{\omega\omega'}^b$ for asymptotically flat black holes. Analytically continuing in ω' then gives

$$\beta_{\omega\omega'}^b \simeq -ie^{-\pi\omega/\kappa_b} \frac{e^{-i\omega/\kappa_c}}{4\pi\kappa_b\sqrt{\omega\omega'}} \left(\frac{i\omega'}{\kappa_b} \right)^{-i\omega/\kappa_b} \left(\Gamma\left(1 + \frac{i\omega}{\kappa_b}\right) + e^{-i\epsilon\pi} \left(\frac{i|\omega'|}{\kappa_b} \right)^\epsilon \Gamma\left(1 - \epsilon + \frac{i\omega}{\kappa_b}\right) \right) \quad (79)$$

Computing the norms of $\alpha_{\omega\omega'}^b$ and $\beta_{\omega\omega'}^b$ shows that the ratio is unchanged from the Schwarzschild case through leading order in ϵ ,

$$|\beta_{\omega\omega'}^b|^2 / |\alpha_{\omega\omega'}^b|^2 = e^{-2\pi\omega/\kappa_b} [1 + \mathcal{O}(\epsilon^2)] \quad (80)$$

Then the normalization property (A6) of the Bogoliubov coefficients gives

$$N_\omega^b \simeq \frac{\gamma_\omega(\epsilon)}{e^{2\pi\omega/\kappa_b} - 1} \quad (81)$$

where $\Gamma_\omega(\epsilon)$ is the classical absorption cross section of the black hole in the SdS spacetime. This elegant result follows because the ratio of the norms (80) is *independent* of ω' , so (A6) reduces to an ω -dependent prefactor times N_ω^b . However, this property does not hold for general black holes, so one has to do the integral over ω' to get the spectrum.

C. Horizon fluctuations and the Schottky anomaly

At the start of this paper we discussed features of the Schottky anomaly for SdS black holes [7], which motivated our choice of modes that are well-behaved on the horizons to define particles. What has been learned about quantum fluctuations in the high and low black hole temperature limits? The large black hole case with $T_b = \kappa_b/2\pi \rightarrow 0$ is the simplest since it is a quasi-equilibrium. Equations (71) and (72) show that the emission is greatly suppressed, and going the next step to compute the energy E_b^ϕ and entropy S_b^ϕ in the field particles gives [7]

$$E_b^\phi \simeq TS_b^\phi \simeq \frac{1}{192\pi^2 l_c} \frac{1}{(2\pi l_c T)^{11/4}} e^{-4/(2\pi l_c T)^{3/4}} \quad (82)$$

and similarly for the cosmological particles. Due to the exponential suppression, the derivatives of n , E_b^ϕ and S_b^ϕ with respect to T_b go to zero as T_b goes to zero. Hence we have shown the fluctuations in energy and entropy due to particle production share the behavior of classical gravitational fluctuations in the low temperature limit.

The $T_b \rightarrow \infty$ limit is more complicated because of the Schwarzschild black hole instability, which persists with nonzero Λ . As is apparent from the increasing number of particles produced as the black hole area goes to zero in (75), the entropy and energy of the produced particles goes to infinity,

$$E_b^\phi = \frac{3T_b}{4} S_b^\phi \simeq \frac{lT_b^2}{27\pi^3} \quad (83)$$

However, a small black hole carries only a small amount of mass and so the emission cuts off after a short amount of time due to back-reaction, which must be taken into account.

Using arguments analogous to the asymptotically flat case, but replacing future null infinity with \mathcal{H}_c^+ , one finds that in Kruskal time ΔU_c the temperature increases by an amount ΔT_b [7]

$$\Delta T_b = \frac{2}{\pi^3} T_b^4 \Delta U_c \quad (84)$$

and that the energy and entropy in produced particles crossing \mathcal{H}_c^+ are [7]

$$\Delta E_b^\phi = \frac{1}{32\pi T_b^2} \Delta T_b, \quad \Delta S_b^\phi = \frac{1}{24\pi T_b^3} \Delta T_b \quad (85)$$

The results (85) are essentially Schwarzschild physics, except that in the asymptotically flat spacetime ΔU_c in (84) is replaced by the change in a null time coordinate at future null infinity. The high temperature limit is complicated because the system is far from equilibrium. The evaporation time scale is fast compared to r_b and l_c , so one needs to look at these dynamical changes in the energy and entropy as T_b changes, and see that they go to zero. Hence energy and entropy fluxes due to particle production are suppressed at high and low temperatures, as is the case for classical fluctuations. It would be interesting to understand for what size black hole the quantum fluxes peak, which is a topic for future work.

D. What about temperatures?

One of the striking features of the particle spectra is that they are not thermal, except for the emission from small black holes. Is this result correct? Recall that both the in and out particle states have been defined with respect to freely falling observers crossing each horizon. On the other hand, if appropriately accelerating observers, namely those who use the Killing time coordinate, are used to define the late time particles then a thermal spectrum does result [12]. These observers have a special status because their time direction is a symmetry direction. However since they are accelerating, they must be equipped with “rockets” to follow their worldlines. This is the case for Rindler observers in Minkowski spacetime who measure a thermal spectrum with temperature proportional to their acceleration, and that calculation is certainly correct. But the Rindler thermal

spectrum results from an extra force that provides the acceleration, rather than reflecting an intrinsic feature of the spacetime geometry. The spectra calculated in this paper describe the particle production measured for observers defined in a natural way near the horizons. The analysis of section (IV A) shows that the non-thermal amplitudes can be expressed as a convolution of two thermal amplitudes, one at temperature $\kappa_b/2\pi$ and one at temperature $\kappa_c/2\pi$.

Beyond the fact that T_b and T_c naturally appear in the first laws for SdS (6) and (7) [13], which extends to slow roll inflation [21] [30] [31], many analyses of the concept of temperature(s) in SdS have been explored in the literature. Researchers have studied several definitions of effective temperature, the role of greybody factors, and different choices of observers [17][18] [19][20] [21] [22] [25][24] [26] [12]. References [20] and [26] attach thermal significance to the radius at which $df/dr = 0$, the former using holographic arguments.

While there is no contradiction in the fact that the spectra calculated in this paper are not thermal, there is a puzzling issue concerning the connection between our particle production results and the temperatures that show up in the first laws (6) and (7) for SdS. These laws relate gravitational perturbations on two different geometrically defined boundaries. The causal diamond first law (7) connects an intersection of the black hole horizon to a space-like related intersection of the cosmological horizon and relies on the existence of the static Killing field. The surface gravities emerge as part of the structure of the horizon geometry. On the other hand, the particle production calculation is done for a scalar field which is added to the system, and no metric perturbations have been included. The first laws do not imply that perturbative matter fields will exhibit thermal properties; and yet one might expect that they “should”. A concrete way of proceeding to elucidate these differences is to note that the particle production process is a measurement on modes that intersect different horizons at locations that are time-like or null related. It could be, for example, that the surface gravity temperatures emerge in correlation functions computed in our state (defined by Kruskal-modes) when the two points are taken close to the black hole horizon or close to the cosmological horizon. This is another topic for future study.

VI. CONCLUSIONS AND FUTURE DIRECTIONS

We have calculated the spectra and integrated fluxes of produced particles crossing each of the future black hole and future cosmological horizons. Near each horizon particle states are defined with respect to the null geodesic, or Kruskal, coordinate there. As a result the particle fluxes are well-behaved on the horizons, but in general the spectra are not thermal. Interestingly, the amplitude for each spectrum can be written as a convolution of two *thermal* amplitudes, one at the cosmological temperature and one at the black hole temperature, weighted by the transmission coefficient for wave propagation in the static SdS coordinates. The convolution integral also leads to the useful result that the geometric optics approximation is a good one if used with a low frequency cut-off determined by where the transmission coefficient changes from zero to one. In the small black limit one recovers a thermal spectrum for the black hole at temperature $\kappa_b/2\pi$, and there is a tiny flux of cosmological particles into the black hole. The large black hole limit is a quasi-equilibrium situation as both temperatures approach the common value of zero and the particle spectra become the same. One finds that the emission derives only from the tail of the distribution and so is exponentially suppressed. As a result, the quantum fluctuations in energy and entropy have the property that $\Delta E^\phi/\Delta T_b$ and $\Delta S^\phi/\Delta T_b$ go to zero as T_b goes to zero. This was one of the conditions needed for the behavior of quantum fluctuations on the horizon to be consistent with the Schottky anomaly behavior of classical gravitational fluctuations. In the small black hole limit, we have argued that after taking into account the dynamical nature of the rapidly evaporating black hole and the small total energy available, one also finds that $\Delta E^\phi/\Delta T_b$ and $\Delta S^\phi/\Delta T_b$ go to zero as $T_b \rightarrow \infty$.

There remain many questions. It would be interesting to understand the emission and absorption for a generic black hole. How big does a black hole have to be to see the effects of Λ ? At what size is the net black hole emission slowed down by a significant factor? Further analysis of the transmission coefficient is required to answer these questions. In this paper we have only used the general feature of $|T_{\nu l}|$. But there could be interesting physics in its behavior at the frequencies picked out by the point of stationary phase. It

is also important understand further of the properties of the state used here, including its two-point function and stress tensor, building on the work of [55][8] to include a black hole, and extending the calculations of [47][17] to beyond the cosmological horizon.

In the times of precision cosmology, one should ask if the signature of primordial black holes during an epoch of inflation could be observed in the cosmic microwave background. A detailed calculation addressing this question was done in [56] using a different state. It would be interesting to extend our calculations to include the behavior of modes in the far field beyond the cosmological horizon, as well as the time dependence of the mass and effective Λ in slow-roll inflation [31], and apply these results to the calculation of quantum fluctuations in inflation. .

Acknowledgements

We would like to thank Paul Anderson, Patrick Draper, David Kastor, and Lorenzo Sorbo for multiple useful conversations. We would also like to thank NORDITA for their hospitality and support during the *Cosmology and Gravitational Physics with Lambda* Scientific Program August 2018, and the Centro de Ciencias de Benasque Pedro Pascual for their hospitality during the *Gravity-New Perspectives from Strings and Higher Dimensions* workshop July 2019. Y.Q. was partially supported by the US-NSF grant PHY-1820675.

APPENDIX

Appendix A: Deriving normalized spectra and rates

To get properly normalized expressions for the quantum spectra and the integrated rates of particle production one needs to use properly normalized wave packets. In terms of the following steps this is equivalent to putting the system in a box of size R^3 so that the

allowed frequencies are integer indexed $\omega_j = j/R$. Since it is not clear what it means to put an SdS black hole in a box, we prefer to think about using normalizable states. The key results are equations (19) and (21) for the particle spectra and the total number of particles produced per unit time expressed in terms of the continuous basis functions, and which depend on the scale R .

To derive these results, let F_j and P_j be normalized wavepackets built out of the f_ω and the p_ω basis modes respectively, so that the packet is peaked at frequencies near $\omega_j = j/R$ [ref-Hawking], where R is a length scale, and normalized as

$$(F_j^h, F_k^h) = \delta_{ij} \ , \quad \text{and} \quad (P_j^h, P_k^h) = \delta_{ij} \tag{A1}$$

The associated creation and annihilation operators satisfy $[a_j^{h\dagger}, a_k^h] = [b_j^{h\dagger}, b_k^h] = \delta_{jk}$, and the field is expanded as

$$\Phi = \sum_{jlm} [P_{jl}^b a_{jl}^b + P_{jl}^c a_{jl}^c + h.c.] = \sum_{jlm} [F_{jl}^b b_{jl}^b + F_{jl}^c b_{jl}^c + h.c.] \tag{A2}$$

Then the two spectra are given by

$$\begin{aligned} N_j^b &= \langle 0 | b_j^{c\dagger} b_j^c | 0 \rangle \ , \quad \text{emission from black hole} \\ N_j^c &= \langle 0 | b_j^{b\dagger} b_j^b | 0 \rangle \ , \quad \text{emission from cosmo horizon} \end{aligned} \tag{A3}$$

The quantities N_j^h are dimensionless. Note that the odd-looking mismatch of labels between the left and right sides of these equations is because, for example, the particle emission interpreted as coming *from* the black hole is measured with the particle operators that are far away from the black hole, in this case the cosmological horizon. The notation “rights itself” in our subsequent expressions (18) for the N_j^h in terms of the Bogoliubov coefficients.

We need to convert the relation (A3) for particle spectra to the basis of continuous functions. Since the commutation relations of the creation and annihilation operators have different dimensions in the two cases, the dimensions of the operators differ, and hence

the dimensions of the mode functions and the Bogoliubov coefficients change as well. The changes in dimensions are summarized by⁶

$$b_j = \frac{1}{\sqrt{R}} b_{\omega_j} , \quad F_j = \frac{1}{\sqrt{R}} f_{\omega_j} , \quad \beta_{jk} = \frac{1}{R} \beta_{\omega_j \omega_k} \quad (\text{A4})$$

The basis expansions (15), (17), and the formulas for the Bogoliubov coefficients (16) become sums over the basis elements,

$$b_j^c = \sum_k \left[\alpha_{jk}^{b*} a_k^b - \beta_{jk}^{b*} a_k^{b\dagger} + A_{jk}^{c*} a_k^c - B_{jk}^{b*} a_k^{c\dagger} \right] \quad (\text{A5})$$

and similarly for the expansions of the other particle operators. We also note the normalization property of the expansion coefficients,

$$\sum_k (|\alpha_{jk}^b|^2 - |\beta_{jk}^b|^2) = 1 - \sum_k (|A_{jk}^b|^2 - |B_{jk}^b|^2) = \gamma^b(\omega_j) \quad (\text{A6})$$

where $\gamma^b(\omega_j)$ is the classical absorption coefficient of the black hole, often referred to as a greybody factor. An analogous relation holds interchanging the indices b and c .

Hence equation (A5) for the probability of horizon h producing a late-time particle with frequency ω_j , in the early-time vacuum state (14), becomes

$$N_{\omega_j}^h = \sum_k |\beta_{jk}^h|^2 , \quad h = b, c \quad (\text{A7})$$

Using (A4) and the relation $\sum_k = R \int d\omega'$, then (A7) becomes

$$N_{\omega}^h = \frac{1}{R} \int d\omega' |\beta_{\omega\omega'}^h|^2 \quad (\text{A8})$$

in the continuous basis. Note the important dimensionful factor of $1/R$ that multiplies the integral using the continuous basis functions, and that N_{ω}^h is dimensionless. This is the desired result.

⁶ These relations are impressionistic in the sense that they hold in converting sums to integrals, but equation (A4) is easier to read.

Appendix B: Stationary Phase to evaluate $\alpha_{\omega\omega'}^b$

The Bogoliubov coefficient (47) can be written as

$$\alpha_{\omega\omega'} = \frac{1}{8\pi^2 \kappa_b \kappa_c \sqrt{\omega\omega'}} \int_0^\infty dx dy e^{-i\omega \frac{y}{\kappa_c}} e^{-i\omega' \frac{x}{\kappa_b}} \int_{-\infty}^\infty d\nu T_\nu^* e^{i\nu(\frac{\ln x}{\kappa_b} + \frac{\ln y}{\kappa_c})} H(x, y, \nu) \quad (\text{B1})$$

where

$$H(x, y, \nu) = \frac{\nu}{xy} + \frac{\omega}{x} + \frac{\omega'}{y} + \frac{\omega\omega'}{\nu}$$

In this appendix we show that two applications of stationary phase bring this multiple integral to the geometric optics form (23) with the important difference that the transmission coefficient is included in the integrand. A third application of stationary phase plus analytic continuation gives the expression for $\beta_{\omega\omega'}^b$ used to get the particle spectra in section (24).

The geometric optics approximation motivates the change of variables $z = yx^\lambda$ with $\lambda = \kappa_c/\kappa_b$ in (B1). This gives our starting point for using stationary phase,

$$\alpha_{\omega\omega'}^b = \frac{1}{8\pi^2 \sqrt{\omega\omega'} \kappa_b \kappa_c} \int_0^\infty dx dz e^{-i\omega z x^{-\lambda}/\kappa_c} e^{-i\omega' x/\kappa_b} \int_{-\infty}^\infty d\nu T_\nu^* H(x, z, \nu) e^{i\nu \ln z/\kappa_c} \quad (\text{B2})$$

where H is now

$$H(x, z, \nu) = \frac{\omega'}{z} + \frac{\omega}{x^{1+\lambda}} + \frac{\nu}{zx} + \frac{\omega\omega'}{\nu x^\lambda} \quad (\text{B3})$$

We first do the integral over z in (B2), taking $\phi(z) = -\omega z x^{-\lambda} + \nu \ln z$. The point of stationary phase is at $z_0 = x^\lambda \nu/\omega$ and using (24) gives

$$\alpha_{\omega\omega'}^b \simeq \frac{\sqrt{2\pi\kappa_c} e^{-\frac{i\pi}{4}}}{8\pi^2 \sqrt{\omega\omega'} \kappa_b \kappa_c} \int_0^\infty dx e^{-i\omega' x/\kappa_b} \frac{x^\lambda}{\omega} \int_{-\infty}^\infty d\nu \sqrt{\nu} T_\nu^* H(x, z_0, \nu) e^{i\nu[-1+\ln(\frac{x^\lambda \nu}{\omega})]/\kappa_c} \quad (\text{B4})$$

Next, take the phase to be $\phi(\nu) = \nu(-1 + \ln(\frac{x^\lambda \nu}{\omega}))$. The stationary point is at $\nu_0 = x^{-\lambda} \omega$, and doing the integral over ν gives

$$\alpha_{\omega\omega'}^b \simeq \frac{1}{2\pi \sqrt{\omega\omega'} \kappa_b} \int_0^\infty dx T_{\nu_0}^* \left(\omega' + \frac{\omega}{x^{1+\lambda}}\right) e^{-i\omega' x/\kappa_b} e^{-ix^{-\lambda} \omega/\kappa_c} \quad (\text{B5})$$

This integrand is the same as the integrand found using the geometric optics approximation, equation (23), with the added ingredient that the transmission coefficient T_ν is in the integrand.

The third application of stationary phase is the same as that used to derive 25) giving

$$\alpha_{\omega\omega'}^b = \frac{\sqrt{2}e^{-i\frac{\pi}{4}} T_{\nu_0}^*}{\sqrt{\pi}\sqrt{\kappa_T}(\omega^{\kappa_c}\omega'^{\kappa_b})^{1/2\kappa_T}} \exp\left[-i\frac{\kappa_T}{\kappa_c\kappa_b}(\omega^{\kappa_c}\omega'^{\kappa_b})^{1/\kappa_T}\right] \quad (\text{B6})$$

where $\nu_0 = (\omega^{\kappa_c}\omega'^{\kappa_b})^{1/\kappa_T}$.

Analytically continuing $\omega' \rightarrow |\omega'|e^{-i\pi}$ as discussed preceding equation (26) gives $\beta_{\omega\omega'}^b$

$$\beta_{\omega\omega'}^b \simeq -i\frac{\sqrt{2}e^{-i\frac{\pi}{4}} e^{i\pi\kappa_b/2\kappa_T}}{\sqrt{\pi}\sqrt{\kappa_T}(\omega^{\kappa_c}\omega'^{\kappa_b})^{1/2\kappa_T}} T_\sigma^* \exp\left[-\frac{\kappa_T}{\kappa_b\kappa_c}(\omega^{\kappa_c}\omega'^{\kappa_b})^{1/\kappa_T} \left(i\cos\pi\frac{\kappa_c}{\kappa_T} + \sin\pi\frac{\kappa_c}{\kappa_T}\right)\right] \quad (\text{B7})$$

where σ is the complex frequency

$$\sigma = (\omega^{\kappa_c}\omega'^{\kappa_b})^{1/\kappa_T} e^{-i\pi\kappa_c/\kappa_T} \quad (\text{B8})$$

Appendix C: Delta function method

As a check on the stationary phase approximation, we use another way to compute the $\alpha_{\omega\omega'}^b$ coefficients. The idea is to replace T_ν with unity in the exact expression, and then show that the difference is subleading. Unfortunately there is one term in (B2) that can not be evaluated by the second method, so this does not fully provide an alternative evaluation.

Rewrite equation B1 as

$$\begin{aligned} \alpha_{\omega\omega'}^b &= \frac{1}{8\pi^2\kappa_b\kappa_c\sqrt{\omega\omega'}} \int_0^\infty dx dy e^{-i\omega\frac{y}{\kappa_c}} e^{-i\omega'\frac{x}{\kappa_b}} \int_{-\infty}^\infty d\nu e^{i\nu(\frac{\ln x}{\kappa_b} + \frac{\ln y}{\kappa_c})} \left(\frac{\nu}{xy} + \frac{\omega}{x} + \frac{\omega'}{y}\right) \\ &\quad + \frac{\sqrt{\omega\omega'}}{8\pi^2\kappa_b\kappa_c} \int_0^\infty dx dy e^{-i\omega\frac{y}{\kappa_c}} e^{-i\omega'\frac{x}{\kappa_b}} \int_{-\infty}^\infty d\nu e^{i\nu(\frac{\ln x}{\kappa_b} + \frac{\ln y}{\kappa_c})} \frac{T_\nu^*}{\nu} \\ &\quad + \frac{1}{8\pi^2\kappa_b\kappa_c\sqrt{\omega\omega'}} \int_0^\infty dx dy e^{-i\omega\frac{y}{\kappa_c}} e^{-i\omega'\frac{x}{\kappa_b}} \int_{-\infty}^\infty d\nu (T_\nu^* - 1) e^{i\nu(\frac{\ln x}{\kappa_b} + \frac{\ln y}{\kappa_c})} \left(\frac{\nu}{xy} + \frac{\omega}{x} + \frac{\omega'}{y}\right) \\ &= \alpha_{\omega\omega'}^{(1)} + \alpha_{\omega\omega'}^{(2)} + \delta\alpha_{\omega\omega'} \end{aligned} \quad (\text{C1})$$

The first term can be simplified by noting that the integral over ν gives delta functions,

$$\begin{aligned}\alpha_{\omega\omega'}^{(1)} &= \frac{1}{4\pi\kappa_b\kappa_c\sqrt{\omega\omega'}} \int_0^\infty dx dy e^{-i\omega\frac{y}{\kappa_c}} e^{-i\omega'\frac{x}{\kappa_b}} \left[\delta'\left(\frac{\ln x}{\kappa_b} + \frac{\ln y}{\kappa_c}\right) \frac{1}{xy} + \delta\left(\frac{\ln x}{\kappa_b} + \frac{\ln y}{\kappa_c}\right) \left(\frac{\omega}{x} + \frac{\omega'}{y}\right) \right] \\ &= \frac{1}{4\pi\kappa_b\sqrt{\omega\omega'}} \int_0^\infty dx e^{-\frac{i\omega x - \lambda}{\kappa_c}} e^{-i\omega'\frac{x}{\kappa_b}} \left(\frac{2\omega}{x^{1+\lambda}} + \omega' \right)\end{aligned}$$

This is almost the result we obtained in the geometric optics limit, but needs a factor of 2 multiplying ω' in the integrand. Turning to $\alpha_{\omega\omega'}^{(2)}$, one again uses successive applications of stationary phase, which gives

$$\alpha_{\omega\omega'}^{(2)} = \frac{1}{4\pi\kappa_b\sqrt{\omega\omega'}} \int_0^\infty dx T_{\nu_0}^* \omega' e^{-\frac{i\omega x - \lambda}{\kappa_c}} e^{-i\omega'\frac{x}{\kappa_b}}$$

Where $\nu_0 = (\omega'^{\kappa_c} \omega^{\kappa_b})^{1/\kappa_T}$. From the analysis in the previous section, we know that since ω and ω' are much greater than ω_0 , ν_0 is also much greater than ω_0 . Hence $T_{\nu_0}^*$ is approximately equal to 1. Then the sum $\alpha_{\omega\omega'}^{(1)} + \alpha_{\omega\omega'}^{(2)}$ is equal to the geometric optics approximation.

To complete the argument we need to check that the magnitude of $\delta\alpha_{\omega\omega'}$ is small. Since $|T_\nu^* - 1| < 1$, $|\delta\alpha_{\omega\omega'}|$, after doing the integral over ν one has

$$\begin{aligned}|\delta\alpha_{\omega\omega'}| &< \left| \frac{1}{8\pi^2\kappa_b\kappa_c\sqrt{\omega\omega'}} \int_0^\infty dx dy e^{-i\omega\frac{y}{\kappa_c}} e^{-i\omega'\frac{x}{\kappa_b}} \left\{ 2i \frac{\sin\left[\omega_0\left(\frac{\ln x}{\kappa_b} + \frac{\ln y}{\kappa_c}\right)\right] - \omega_0\left(\frac{\ln x}{\kappa_b} + \frac{\ln y}{\kappa_c}\right) \cos\left[\omega_0\left(\frac{\ln x}{\kappa_b} + \frac{\ln y}{\kappa_c}\right)\right]}{xy\left(\frac{\ln x}{\kappa_b} + \frac{\ln y}{\kappa_c}\right)^2} \right. \right. \\ &\quad \left. \left. + \frac{2\sin\left[\omega_0\left(\frac{\ln x}{\kappa_b} + \frac{\ln y}{\kappa_c}\right)\right]}{\left(\frac{\ln x}{\kappa_b} + \frac{\ln y}{\kappa_c}\right)} \left(\frac{\omega}{x} + \frac{\omega'}{y}\right) \right\} \right| \\ &\approx \left| \frac{e^{-i\omega_0\left(\frac{1}{\kappa_c} + \frac{1}{\kappa_b}\right)}}{2\pi z\sqrt{\kappa_b\kappa_c\omega\omega'}} \left[\frac{\sin(\omega_0 z)}{\omega_0 z} - \cos(\omega_0 z) - 2i\sin(\omega_0 z) \right] \right| \quad (C2)\end{aligned}$$

where stationary phase approximation has been used to do the integrals over x and y and

$z = \frac{1}{\kappa_b} \ln(\frac{\omega_0}{\omega'}) + \frac{1}{\kappa_c} \ln(\frac{\omega_0}{\omega})$. So the ratio is approximately equal to

$$\frac{|\delta\alpha_{\omega\omega'}|^2}{|\alpha_{\omega\omega'}^b|^2} \simeq \frac{\kappa_T}{8\pi\kappa_b\kappa_c\omega^{\kappa_b/\kappa_T}\omega'^{\kappa_c/\kappa_T}z^2} \left[\left(\frac{\sin(\omega_0 z)}{\omega_0 z} - \cos(\omega_0 z) \right)^2 + 4\sin^2(\omega_0 z) \right] \quad (\text{C3})$$

For ω and ω' much greater than the cutoff, $z \rightarrow -\infty$, which gives $\frac{|\delta\alpha_{\omega\omega'}|^2}{|\alpha_{\omega\omega'}^b|^2} \rightarrow 0$. Hence the contribution from $\delta\alpha_{\omega\omega'}$ is small compared to $\alpha_{\omega\omega'}^{(1)}$ and $\alpha_{\omega\omega'}^{(2)}$. To summarize, replacing T_ν by one in (C1), one can evaluate three of the four terms by Fourier transforms. The fourth term contains the factor T_ν/ν which is well behaved as ν goes to zero since T_ν vanishes, so it is not useful to put $T_\nu = 1$ since that introduces an artificial singularity, and stationary phase was used instead. The correction term $\delta\alpha_{\omega\omega'}$ is small compared to the geometric optics result. Note that a more precise analysis of the the low frequency behavior of the transmission coefficient could allow a better approximation to the fourth term.

Appendix D: Energy and entropy of produced particles

The particle spectra and total emission rates are given in equations (66) to (70). The energy fluxes in the particles are given by

$$\begin{aligned} E_c &= \int_{\omega_1} d\omega \omega^3 r_b^2 N_\omega^c \\ &= \frac{4r_b^2}{4\pi R \sin(\frac{\pi}{\epsilon+1})} \left[\frac{\epsilon\kappa_b}{2(1+\epsilon)\sin(\frac{\pi}{\epsilon+1})} \right]^{\frac{3}{\epsilon}+3} \omega_0^{-\frac{3}{\epsilon}} \Gamma\left(\frac{3}{\epsilon} + 3, \frac{\omega_0^{\kappa_b/\kappa_T} \omega_1^{\kappa_c/\kappa_T}}{\mathcal{K}}\right) \end{aligned} \quad (\text{D1})$$

and

$$\begin{aligned} E_b &= \frac{A}{4\pi} \int_{\omega_1} d\omega \omega^2 N_\omega^b \\ &= \frac{A\omega_0^{-\frac{3\kappa_c}{\kappa_b}}}{4\pi^2 R \sin(\pi\kappa_c/\kappa_T)} \mathcal{K}^{\frac{3\kappa_T}{\kappa_b}} \Gamma\left(\frac{3\kappa_T}{\kappa_b}, \frac{\omega_0^{\kappa_c/\kappa_T} \omega_1^{\kappa_b/\kappa_T}}{\mathcal{K}}\right) \end{aligned} \quad (\text{D2})$$

where $\epsilon = \kappa_b/\kappa_c$ is not necessarily small in these expressions.

For small black holes take $\epsilon \ll 1$ limit and use $\omega_0 = \omega_1 = \kappa_b/2\pi$,

$$E_b \approx \frac{\kappa_b^2}{108\pi^5} \Gamma(3, 1) \quad (\text{D3})$$

which gives equation (83). For large black holes, take the limit $\epsilon \rightarrow 1$ with $\omega_0 = \kappa^{3/2}l^{1/2}$, $\omega_1 = \frac{1}{\kappa l^2}$, and $R = \kappa l_c^2$. One obtains

$$E_c \rightarrow E_b = E \approx \frac{A\kappa^{1/2}}{4^7\pi l_c^{7/2}} \Gamma\left(6, \frac{4}{(\kappa l_c)^{3/4}}\right) \quad (\text{D4})$$

which then gives equation (82). The entropy in the produced particles comes from using the first law $dE = TdS$ [7].

-
- [1] J. M. Bardeen, B. Carter and S. W. Hawking, “The Four laws of black hole mechanics,” *Commun. Math. Phys.* **31**, 161 (1973). doi:10.1007/BF01645742
 - [2] S. W. Hawking, “Particle Creation by Black Holes,” *Commun. Math. Phys.* **43**, 199 (1975)
Erratum: [*Commun. Math. Phys.* **46**, 206 (1976)].
 - [3] G. W. Gibbons and S. W. Hawking, “Cosmological Event Horizons, Thermodynamics, and Particle Creation,” *Phys. Rev. D* **15**, 2738 (1977). doi:10.1103/PhysRevD.15.2738
 - [4] D. Kastor and J. H. Traschen, “Particle production and positive energy theorems for charged black holes in De Sitter,” *Class. Quant. Grav.* **13**, 2753 (1996) doi:10.1088/0264-9381/13/10/013 [gr-qc/9311025].
 - [5] W. G. Unruh, “Notes on black hole evaporation,” *Phys. Rev. D* **14**, 870 (1976). doi:10.1103/PhysRevD.14.870
 - [6] R. Balbinot and R. Bergamini, “Quantum State For A Black Hole In A De Sitter Universe,” *Lett. Nuovo Cim.* **44**, 423 (1985).

- [7] J. Dinsmore, P. Draper, D. Kastor, Y. Qiu and J. Traschen, “Schottky Anomaly of deSitter Black Holes,” arXiv:1907.00248 [hep-th].
- [8] L. Aalsma, M. Parikh and J. P. Van Der Schaar, “Back(reaction) to the Future in the Unruh-de Sitter State,” arXiv:1905.02714 [hep-th].
- [9] C. V. Johnson, “Specific Heats and Schottky Peaks for Black Holes in Extended Thermodynamics,” arXiv:1905.00539 [hep-th].
- [10] C. V. Johnson, “de Sitter Black Holes, Schottky Peaks, and Continuous Heat Engines,” arXiv:1907.05883 [hep-th].
- [11] D. Grumiller, R. McNees and J. Salzer, “Cosmological constant as confining U(1) charge in two-dimensional dilaton gravity,” Phys. Rev. D **90**, no. 4, 044032 (2014) doi:10.1103/PhysRevD.90.044032 [arXiv:1406.7007 [hep-th]].
- [12] S. Bhattacharya, “Particle creation by de Sitter black holes revisited,” Phys. Rev. D **98**, no. 12, 125013 (2018) doi:10.1103/PhysRevD.98.125013 [arXiv:1810.13260 [gr-qc]].
- [13] B. P. Dolan, D. Kastor, D. Kubiznak, R. B. Mann and J. Traschen, “Thermodynamic Volumes and Isoperimetric Inequalities for de Sitter Black Holes,” Phys. Rev. D **87**, no. 10, 104017 (2013) doi:10.1103/PhysRevD.87.104017 [arXiv:1301.5926 [hep-th]].
- [14] M. H. Dehghani and H. KhajehAzad, “Thermodynamics of Kerr-Newman de Sitter black hole and dS / CFT correspondence,” Can. J. Phys. **81**, 1363 (2003) doi:10.1139/p03-110 [hep-th/0209203].
- [15] S. Shankaranarayanan, “Temperature and entropy of Schwarzschild-de Sitter space-time,” Phys. Rev. D **67**, 084026 (2003) doi:10.1103/PhysRevD.67.084026 [gr-qc/0301090].
- [16] M. R. Medrano and N. G. Sanchez, “Semiclassical and Quantum Black Holes and their Evaporation, de Sitter and Anti-de Sitter Regimes, Gravitational and String Phase Transitions,” Int. J. Mod. Phys. A **22**, 6089 (2007) doi:10.1142/S0217751X07038669 [arXiv:0712.0727 [hep-th]].
- [17] T. R. Choudhury and T. Padmanabhan, “Concept of temperature in multi-horizon spacetimes: Analysis of Schwarzschild-de Sitter metric,” Gen. Rel. Grav. **39**, 1789 (2007) doi:10.1007/s10714-007-0489-0 [gr-qc/0404091].
- [18] Y. S. Myung, “Thermodynamics of the Schwarzschild-de Sitter black hole: Thermal stability

- of the Nariai black hole,” *Phys. Rev. D* **77**, 104007 (2008) doi:10.1103/PhysRevD.77.104007 [arXiv:0712.3315 [gr-qc]].
- [19] M. Urano, A. Tomimatsu and H. Saida, “Mechanical First Law of Black Hole Spacetimes with Cosmological Constant and Its Application to Schwarzschild-de Sitter Spacetime,” *Class. Quant. Grav.* **26**, 105010 (2009) doi:10.1088/0264-9381/26/10/105010 [arXiv:0903.4230 [gr-qc]].
- [20] E. Chang-Young, M. Eune, K. Kimm and D. Lee, “Schwarzschild-de Sitter black hole from entropic viewpoint,” *Mod. Phys. Lett. A* **26**, 1975 (2011) doi:10.1142/S0217732311036450 [arXiv:1011.3960 [hep-th]].
- [21] S. W. Kim, “The Hawking temperature of a dynamical black hole in de Sitter spacetime,” *Grav. Cosmol.* **20**, no. 4, 247 (2014). doi:10.1134/S0202289314040094
- [22] N. Ishwarchandra and K. Y. Singh, “Vaidya black hole in non-stationary de Sitter space: Hawking’s temperature,” *Astrophys. Space Sci.* **350**, 285 (2014)
- [23] S. Bhattacharya, “A note on entropy of de Sitter black holes,” *Eur. Phys. J. C* **76**, no. 3, 112 (2016) doi:10.1140/epjc/s10052-016-3955-6 [arXiv:1506.07809 [gr-qc]].
- [24] H. F. Li, M. S. Ma and Y. Q. Ma, “Thermodynamic properties of black holes in de Sitter space,” *Mod. Phys. Lett. A* **32**, no. 02, 1750017 (2016) doi:10.1142/S0217732317500171 [arXiv:1605.08225 [hep-th]].
- [25] K. Hajian, “Conserved charges and first law of thermodynamics for Kerr-de Sitter black holes,” *Gen. Rel. Grav.* **48**, no. 8, 114 (2016) doi:10.1007/s10714-016-2108-4 [arXiv:1602.05575 [gr-qc]].
- [26] T. Pappas and P. Kanti, “Schwarzschild-de Sitter spacetime: The role of temperature in the emission of Hawking radiation,” *Phys. Lett. B* **775**, 140 (2017) doi:10.1016/j.physletb.2017.10.058 [arXiv:1707.04900 [hep-th]].
- [27] P. Kanti and T. Pappas, “Effective temperatures and radiation spectra for a higher-dimensional Schwarzschild-de Sitter black hole,” *Phys. Rev. D* **96**, no. 2, 024038 (2017) doi:10.1103/PhysRevD.96.024038 [arXiv:1705.09108 [hep-th]].
- [28] C. W. Robson, L. D. M. Villari and F. Biancalana, “Global Hawking Temperature of Schwarzschild-de Sitter Spacetime: a Topological Approach,” arXiv:1902.02547 [gr-qc].

- [29] D. Klemm and M. Nozawa, “Black holes in an expanding universe and supersymmetry,” *Phys. Lett. B* **753**, 110 (2016) doi:10.1016/j.physletb.2015.12.006 [arXiv:1511.01949 [hep-th]].
- [30] R. Gregory, D. Kastor and J. Traschen, “Black Hole Thermodynamics with Dynamical Lambda,” *JHEP* **1710**, 118 (2017) doi:10.1007/JHEP10(2017)118 [arXiv:1707.06586 [hep-th]].
- [31] R. Gregory, D. Kastor and J. Traschen, “Evolving Black Holes in Inflation,” *Class. Quant. Grav.* **35**, no. 15, 155008 (2018) doi:10.1088/1361-6382/aacec2 [arXiv:1804.03462 [hep-th]].
- [32] N. D. Birrell and P. C. Davies *Quantum Fields in Curved Space*, Cambridge University Press, Cambridge (1982).
- [33] J. H. Traschen, “An Introduction to black hole evaporation,” gr-qc/0010055.
- [34] B. S. DeWitt, “Quantum Field Theory in Curved Space-Time,” *Phys. Rept.* **19**, 295 (1975). doi:10.1016/0370-1573(75)90051-4
- [35] W. Z. Chao, “Quantum fields in Schwarzschild-de Sitter space,” *Int. J. Mod. Phys. D* **7**, 887 (1998) doi:10.1142/S0218271898000589 [gr-qc/9712066].
- [36] E. Mottola, “Particle Creation in de Sitter Space,” *Phys. Rev. D* **31**, 754 (1985). doi:10.1103/PhysRevD.31.754
- [37] J. H. Traschen and C. T. Hill, “Instability of De Sitter Space on Short Time Scales,” *Phys. Rev. D* **33**, 3519 (1986). doi:10.1103/PhysRevD.33.3519
- [38] P. R. Anderson, W. Eaker, S. Habib, C. Molina-Paris and E. Mottola, “Attractor states and infrared scaling in de Sitter space,” *Phys. Rev. D* **62**, 124019 (2000) doi:10.1103/PhysRevD.62.124019 [gr-qc/0005102].
- [39] P. R. Anderson, W. Eaker, S. Habib, C. Molina-Paris and E. Mottola, “Attractor states and quantum instabilities in de Sitter space,” *Int. J. Theor. Phys.* **40**, 2217 (2001). doi:10.1023/A:1012934204432
- [40] H. Collins, R. Holman and M. R. Martin, “The Fate of the alpha vacuum,” *Phys. Rev. D* **68**, 124012 (2003) doi:10.1103/PhysRevD.68.124012 [hep-th/0306028].
- [41] H. Collins and R. Holman, “Taming the alpha vacuum,” *Phys. Rev. D* **70**, 084019 (2004) doi:10.1103/PhysRevD.70.084019 [hep-th/0312143].
- [42] K. E. Leonard, T. Prokopec and R. P. Woodard, “Covariant Vacuum Polarizations on de

- Sitter Background,” *Phys. Rev. D* **87**, no. 4, 044030 (2013) doi:10.1103/PhysRevD.87.044030 [arXiv:1210.6968 [gr-qc]].
- [43] K. E. Leonard, T. Prokopec and R. P. Woodard, “Representing the Vacuum Polarization on de Sitter,” *J. Math. Phys.* **54**, 032301 (2013) doi:10.1063/1.4793987 [arXiv:1211.1342 [gr-qc]].
- [44] P. R. Anderson and E. Mottola, “Quantum vacuum instability of ’Eternal’ de Sitter space,” *Phys. Rev. D* **89**, 104039 (2014) doi:10.1103/PhysRevD.89.104039 [arXiv:1310.1963 [gr-qc]].
- [45] T. Markkanen, “De Sitter Stability and Coarse Graining,” *Eur. Phys. J. C* **78**, no. 2, 97 (2018) doi:10.1140/epjc/s10052-018-5575-9 [arXiv:1703.06898 [gr-qc]].
- [46] A. Das, S. Dalui, C. Chowdhury and B. R. Majhi, “Conformal Vacuum and Fluctuation-Dissipation in de-Sitter Universe and Black Hole Spacetimes,” arXiv:1902.03735 [gr-qc].
- [47] D. Markovic and W. G. Unruh, “Vacuum for a massless scalar field outside a collapsing body in de Sitter space-time,” *Phys. Rev. D* **43** (1991) 332. doi:10.1103/PhysRevD.43.332
- [48] K. Chakraborty and B. R. Majhi, “Detector response along null geodesics in black hole spacetimes and in a Friedmann-Lemaitre-Robertson-Walker Universe,” arXiv:1905.10554 [gr-qc].
- [49] R. Bousso and S. W. Hawking, “(Anti)evaporation of Schwarzschild-de Sitter black holes,” *Phys. Rev. D* **57**, 2436 (1998) doi:10.1103/PhysRevD.57.2436 [hep-th/9709224].
- [50] H. Ghafarnejad, “Stability of the evaporating Schwarzschild-de Sitter black hole final state,” *Phys. Rev. D* **74**, 104012 (2006). doi:10.1103/PhysRevD.74.104012
- [51] Q. Q. Jiang, “Hawking radiation from black holes in de Sitter spaces,” *Class. Quant. Grav.* **24**, 4391 (2007) doi:10.1088/0264-9381/24/17/008 [arXiv:0705.2068 [hep-th]].
- [52]
- [52] S. Bhattacharya and A. Lahiri, “Mass function and particle creation in Schwarzschild-de Sitter spacetime,” *Eur. Phys. J. C* **73**, 2673 (2013) doi:10.1140/epjc/s10052-013-2673-6 [arXiv:1301.4532 [gr-qc]].
- [53] P. Kanti, T. Pappas and N. Pappas, “Greybody factors for scalar fields emitted by a higher-dimensional Schwarzschild-de Sitter black hole,” *Phys. Rev. D* **90**, no. 12, 124077 (2014) doi:10.1103/PhysRevD.90.124077 [arXiv:1409.8664 [hep-th]].
- [54] T. Pappas, P. Kanti and N. Pappas, “Hawking radiation spectra for scalar fields by a higher-

- dimensional Schwarzschild-de Sitter black hole,” *Phys. Rev. D* **94**, no. 2, 024035 (2016) doi:10.1103/PhysRevD.94.024035 [arXiv:1604.08617 [hep-th]].
- [55] J. D. Bates, H. T. Cho, P. R. Anderson and B. L. Hu, “Noise kernel near the horizon of de Sitter space,” *Class. Quant. Grav.* **31**, 025015 (2014). doi:10.1088/0264-9381/31/2/025015
- [56] T. Prokopec and P. Reska, “Scalar cosmological perturbations from inflationary black holes,” *JCAP* **1103**, 050 (2011) doi:10.1088/1475-7516/2011/03/050 [arXiv:1007.3851 [gr-qc]].